Quaternary Science Reviews 89 (2014) 13–26

Contents lists available at ScienceDirect

Quaternary Science Reviews

journal homepage: www.elsevier.com/locate/quascirev

Using silicon isotopes to understand the role of the Southern Ocean in modern and ancient biogeochemistry and climate

Katharine R. Hendry [a,b,*], Mark A. Brzezinski [c,d]

[a] School of Earth and Ocean Sciences, Cardiff University, Park Place, Cardiff CF10 3AT, UK
[b] School of Earth Sciences, University of Bristol, Wills Memorial Building, Queen's Road, Bristol BS8 1RJ, UK
[c] Department of Ecology Evolution and Marine, Marine Sciences Institute, University of California, Santa Barbara, CA 93106-6150, USA
[d] Marine Science Institute, University of California, Santa Barbara, CA 93106-6150, USA

ARTICLE INFO

Article history:
Received 24 September 2013
Received in revised form
16 January 2014
Accepted 30 January 2014
Available online 3 March 2014

Keywords:
Silicon isotope
Silicic acid
Opal
Diatom

ABSTRACT

The growth of siliceous phytoplankton, mainly diatoms, in the Southern Ocean influences the preformed nutrient inventory in the ocean on a global scale. Silicic acid use by diatoms and deep circulation combine to trap dissolved Si in the Southern Ocean resulting in high levels of silica production and expansive diatom oozes in Southern Ocean sediments. The analysis of the silicon isotope composition of biogenic silica, or opal, and dissolved silicic acid provide insight into the operation of the global marine silicon cycle and the role played by the Southern Ocean in nutrient supply and carbon drawdown, both in the modern and in the past. Silicon isotope studies of diatoms have provided insight into the history of silica production in surface waters, while the analysis of spicules from deep sea sponges has defined both the spatial and the temporal variability of silicic acid concentrations in the water column; together these – and other – proxies reveal variations in the northward flow of Southern Ocean intermediate and mode waters and how changes in Southern Ocean productivity altered their preformed nutrient content. We present a new hypothesis – the "Silicic Acid Ventilation Hypothesis" (SAVH) – to explain the geographical variation of opal-based proxy records, in particular the contrasting patterns of opal burial change found in the low and high latitudes. By understanding the silicon isotope systematics of opal and silicic acid in the modern, we will be able to use opal-based proxies to reconstruct past changes in the Southern Ocean and so investigate its role in global carbon cycling and climate.

1. Introduction

1.1. Background and motivation

The Southern Ocean plays a central role in governing the inventory of preformed nutrients and carbon storage in the global ocean (Marinov et al., 2006, 2008). Of particular interest is the role of Southern Ocean circulation and biogeochemistry as a major control on the global distribution of the dissolved silicon – silicic acid or $Si(OH)_4$ – and as the single largest locus of modern opal deposition on the sea floor (Cortese et al., 2004, Fig. 1). The formation and burial of biogenic opal, amorphous silica, is the most important sink of $Si(OH)_4$ in the modern oceans, and is formed predominantly by diatoms, a diverse group of photosynthetic protists from the Class Bacillariophyceae. Diatoms have an absolute requirement for $Si(OH)_4$ and have evolved mechanisms for efficient Si uptake and metabolism (Martin-Jezequel et al., 2003). $Si(OH)_4$ uptake by diatoms severely depletes dissolved Si from surface waters (Falkowski et al., 2004). As such, diatoms rely on upwelled waters with elevated $Si(OH)_4$, thriving in ecosystems such as coastal and open ocean upwelling zones, areas of deep winter mixing (such as the Southern Ocean frontal zones), and – in the case of some giant diatoms – obtaining their requisite silicon from deep nutriclines in highly stratified waters (Kemp et al., 2006).

Diatoms contribute up to 40% of global marine primary productivity, and approximately half of the opal produced in the euphotic zone is exported to deep waters (Nelson et al., 1995; Tréguer et al., 1995). Approximately 3% of biogenic opal production is preserved in ocean floor sediments as a global average (Nelson et al., 1995), with the remainder remineralized in the water column or at the sediment–water interface (reviewed by Tréguer and De la Rocha, 2013). Although the Southern Ocean is the single largest site of opal deposition (the "opal belt") in the modern

* Corresponding author. School of Earth Sciences, University of Bristol, Wills Memorial Building, Queen's Road, Bristol BS8 1RK, UK. Tel.: +44 (0)117 954 5379.
E-mail address: K.Hendry@bristol.ac.uk (K.R. Hendry).

http://dx.doi.org/10.1016/j.quascirev.2014.01.019
0277-3791/

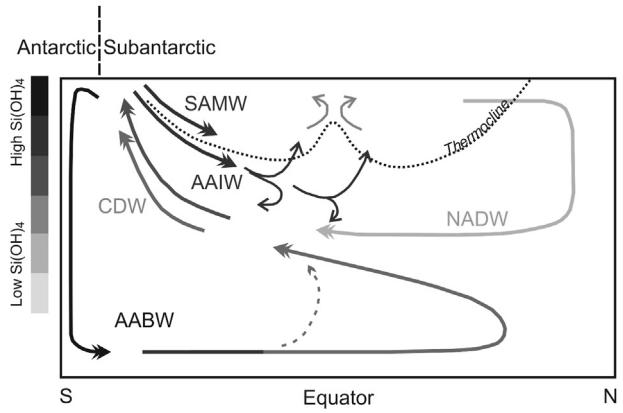

Fig. 1. Schematic of the transport of $Si(OH)_4$ in the ocean and the relationship with the MOC, after Marinov et al. (2008). The double-headed arrows show the major water masses, shaded according to $Si(OH)_4$ concentration. The dashed line shows the thermocline depth.

ocean (Cortese et al., 2004), opal preservation efficiency in the Southern Ocean is not significantly different from the global average (2–6%; DeMaster, 2002; Nelson et al., 2002; Pondaven et al., 2000) such that the high opal accumulation rates in Southern Ocean sediments is sustained by high rates of opal production rather than high preservation efficiency.

Diatom opal has received significant scrutiny over the past decades as a source of paleoceanographic information. Southern Ocean waters are often too corrosive for the preservation of traditional carbonate proxies, creating substantial interest in using opal as an indicator of past changes in southern component water. Opal accumulation rates, when ^{230}Th − normalised to account for sediment redistribution, provide an important constraint on the productivity and export of diatoms from surface waters into deep waters and sediments (Chase et al., 2003b). ^{231}Pa/^{230}Th ratios in opal-rich regions provide an additional constraint on opal production, versus preservation, due to the affinity of ^{231}Pa for opal (Chase et al., 2002). Given the dependence of diatoms on deep sources of $Si(OH)_4$, ^{230}Th-normalised opal accumulation rates, paired with ^{231}Pa/^{230}Th ratios, have been used as a proxy for wind-driven upwelling in the Southern Ocean (Anderson et al., 2009).

In addition to opal accumulation, there has been an increasing interest in the last twenty years on the use of aspects of opal chemistry as biogeochemical proxies for environmental conditions and productivity, including elemental ratios of occluded trace constituents (Ellwood and Hunter, 1999; Lal et al., 2006; Hendry and Rickaby, 2008) and stable isotopes of Si (De La Rocha et al., 1997; De La Rocha et al., 1998), O (Shemesh, 1995; Leng and Sloane, 2008), and more recently Zn (Andersen et al., 2011; Hendry and Andersen, 2013). One of the widest used applications is that of Si isotope analysis of diatom opal as a proxy for silica production. Briefly, there are three naturally occurring stable isotopes of silicon, ^{28}Si (~92 atom %), ^{29}Si (~5 atom %) and ^{30}Si (~3 atom %), and the silicon isotope composition of a material is denoted by δ^{30}Si, where:

$$\delta^{30}\mathrm{Si} = \left[\left(^{30}\mathrm{Si}/^{28}\mathrm{Si}\right)_{\mathrm{sample}}/\left(^{30}\mathrm{Si}/^{28}\mathrm{Si}\right)_{\mathrm{standard-NBS28}} - 1\right] \times 1000 \quad (1)$$

De La Rocha and co-workers first reported on the fractionation of isotopes of Si by diatoms using laboratory cultures (De La Rocha et al., 1997). That work indicated that diatoms have a constant fractionation factor (ε) favouring the lighter isotope ^{28}Si over ^{30}Si by ~1.1‰, with similar results achieved a few years later in further culture studies (Milligan et al., 2004) and field observations of water column diatoms (Varela et al., 2004; Fripiat et al., 2011, 2012), but see Sutton et al. (2013) for evidence for possible interspecific variation in ε (see below). Hence, as $Si(OH)_4$ utilization increases, both dissolved silicic acid and the opal produced from it become progressively enriched in the heavier isotopes of Si, such that the silicon isotopic composition of diatom opal extracted from dated sediment cores can be used as a measure of past surface ocean Si utilization. These concepts were first applied to downcore records of diatom δ^{30}Si from the Southern Ocean (De La Rocha et al., 1998). This progressive fractionation can be modeled as a Rayleigh-type closed distillation process, or a steady state open system, assuming a constant value of ε and a known starting isotopic composition of the nutrient substrate (De La Rocha et al., 1997; Varela et al., 2004).

The aim of this review is to bring together advances in oceanic silicon isotope studies with a focus on the role of Southern Ocean circulation and productivity in controlling the global distribution of $Si(OH)_4$ and the contribution of diatoms to global marine productivity. We will explore controls on Si isotope distribution deduced from models of modern oceanic $\delta^{30}Si(OH)_4$ distributions, the application of Si isotopes to paleoceanographic studies of Earth's climate, using the Silicic Acid Leakage Hypothesis (SALH) as a case study, and the future of opal-based multi-proxy approaches in paleoceanography.

2. Silicon isotopes as a silica production proxy

2.1. Culture experiments on diatoms

Since the original studies of De La Rocha et al. (1997) and Milligan et al. (2004), there was a considerable gap before further laboratory culture studies were carried out, which ended only recently with the publication of new culture experiments by Sutton et al. (2013). These culture experiments used the same species as the original studies (*Thalassiosira weissflogii* and *Thalassiosira pseudonana*, De La Rocha et al., 1997; Milligan et al., 2004), and some Southern Ocean species that had not been previously studied (*Porosira glacilis*, *Thalassiosira antarctica*, *Thalassiosira nordenskioeldii*, *Fragilariopsis kerguelensis*, *Chaeotceros brevis*). Most of the results were consistent with the original findings (Fig. 2), supporting the paradigm that diatom ε has a value of −1.1‰ within experimental uncertainty. However, there were some discrepancies between the different studies for different strains of the same species, *T. weissflogii*. Furthermore, two polar species had significantly different fractionation factors: *F. kerguelensis* showed a ε value of −0.54‰ (mean for two strains) and *C. brevis* showed a ε value of −2.09‰ (Sutton et al., 2013). Two major questions arising from these studies are: Do the results of culture experiments capture the range of fractionation by diatoms in the natural environment? And, is interspecific variation in ε, as represented by the extreme value for *C. brevis*, detectable in nature?

2.2. Proxy verification: core top calibrations of diatoms

2.2.1. Cleaning methods

An important aspect of paleoceanographic applications of opal composition is the effective cleaning of frustules to remove clays and fragments of other biogenic opal producers (radiolarians, sponge spicules). Heavy liquid separation has been used routinely for opal analysis for over twenty years, but there are numerous different approaches for further physical and chemical cleaning of the opal prior to analysis (Shemesh, 1989; Ellwood and Hunter, 1999; Lal et al., 2006; Hendry and Rickaby, 2008). Most studies of diatom Si isotopes have employed variants on these more

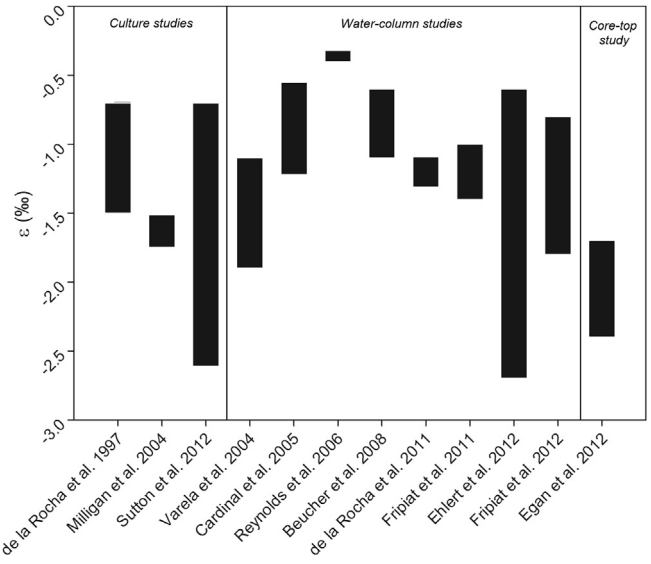

Fig. 2. Apparent fractionation factors estimated from a number of culture, water column and sediment core top studies (De La Rocha et al., 1997; Milligan et al., 2004; Varela et al., 2004; Cardinal et al., 2005; Reynolds et al., 2006; Beucher et al., 2008; De La Rocha et al., 2011; Fripiat et al., 2011; Cao et al., 2012; Egan et al., 2012; Fripiat et al., 2012; Ehlert et al., 2013; Sutton et al., 2013).

traditional methods. Most recently, a microfiltration method originally designed to separate different species of coccoliths from sediments (Minoletti et al., 2009) has recently been adapted for the cleaning and separation of different size fractions of opal (Egan et al., 2012). The gentle sonication of the samples limits the potential for frustule fragmentation and thus mechanical loss of material. The studies show that size fractions for core tops in the Southern Ocean between 2 and 20 μm contain only clean diatom opal and yield reproducible δ^{30}Si values. Fractions below and above this range show $\Delta\delta^{30}$Si offsets: <2 μm contain unidentifiable fragments whereas fractions >20 μm contain identifiable fragments of sponge spicules and radiolarians.

There are some potential issues relating to size fractionation of opal samples. Firstly, although the microfiltration method is designed to limit the fragmentation and loss of material, it is still inevitable that material will be lost during the heavy liquid separation stage, any further filtration stages and during chemical cleaning. Secondly, selective loss of more fragile frustules, and size selection of different species, may both reduce apparent variability and introduce a bias into the measurement, for example, towards species that grow at a particular time of year or a particular ambient $Si(OH)_4$ condition. However, the few studies that have been carried out on hand-picked individual frustules of particular species have shown little offset with bulk opal δ^{30}Si values (e.g. Hendry et al., in press).

2.2.2. Core top calibration results

As alluded to above, one key point to address is whether the opal δ^{30}Si signal from diatoms in the upper parts of the water column is preserved with fidelity in the sediments. To address this Egan et al. (2012) carried out the first core top calibration of diatom δ^{30}Si using the microfiltration method. The authors found a good correspondence between the core top diatom δ^{30}Si from the 2–20 μm size fraction and the minimum annual $Si(OH)_4$ in the overlying surface waters, which, assuming the same initial $Si(OH)_4$ concentration everywhere at the end of winter should reflect the extent of $Si(OH)_4$ depletion. This result suggests that the sedimentary signal reflects the cumulative seasonal drawdown of $Si(OH)_4$ supporting the use of δ^{30}Si as a production proxy (Egan et al., 2012). Moreover, these data imply that species composition does not impact the δ^{30}Si, once the opal from radiolarians and sponge spicules has been removed. The calculated ε values from the core tops appear to be greater when modelled at steady state from a single source of water (Fig. 2). However, the core top results are compatible with an ε value of −1.1‰ if fractionation occurs from waters with a $\delta^{30}Si(OH)_4$ composition that lies on a mixing line representing a varying mixture of isotopically heavy surface water and lighter deep water in the Southern Ocean (Egan et al., 2012).

2.3. Field estimates of the Si fractionation factor

Field estimates of the fractionation factor ε have been made using either the gradient in the isotopic composition of silicic acid across the nutricline, or from the difference between the isotopic composition of co-located samples of biogenic silica and dissolved silicon. Nutrient and isotope profiles can be used to estimate isotope fractionation using either an open system model (continuous delivery of Si into the euphotic zone) or a closed system model (assuming one isolated pulse of Si delivered into the euphotic zone followed by closed system dynamics) depending on the nature of the vertical nutrient supply. These models are described by the following equations:

$$\text{Open}: \delta^{30}Si(OH)_{4observed} = \delta^{30}Si(OH)_{4initial} - \varepsilon^*(1-f) \quad (2a)$$

$$\text{Closed}: \delta^{30}Si(OH)_{4observed} = \delta^{30}Si(OH)_{4initial} + \varepsilon^*\ln(f) \quad (2b)$$

where $\delta^{30}Si(OH)_{4observed}$ is the measured $\delta^{30}Si(OH)_4$ in surface waters, $\delta^{30}Si(OH)_{4initial}$ is that of the water mass supplying Si to surface waters and f is the fraction of the supply that remains in surface waters. Simple algebra can be used to show that surface water $\delta^{30}Si(OH)_4$ should be a linear function of $[Si(OH)_4]_{observed}/[Si(OH)_4]_{initial}$ (open) or $\ln[Si(OH)_4]_{observed}$ (closed) with a slope equal to ε (Varela et al., 2004).

In both the open and closed isotope models the $\delta^{30}Si(OH)_4$ of waters ventilating to the surface is required. Uncertainty in this value has led to considerable variations in estimates of ε (Reynolds et al., 2006) inspiring efforts to better understand $\delta^{30}Si(OH)_4$ distributions in subsurface waters.

In principle, ε can also be estimated from the difference between δ^{30}Si of opal and $\delta^{30}Si(OH)_4$, a parameter denoted by $\Delta\delta^{30}$Si (Cardinal et al., 2005; Fripiat et al., 2007; De La Rocha et al., 2011). Equating $\Delta\delta^{30}$Si and ε is only approximate due to the influence of vertical mixing of isotopically light $Si(OH)_4$ altering the biologically-driven relationship between δ^{30}Si of opal and $\delta^{30}Si(OH)_4$.

A summary of the values of ε from field programs is given in Fig. 2. The range of estimated fractionation factors reflects both real-world variation in ε and methodological challenges. Often the simple assumptions made when applying isotope models are violated in natural systems. No system is entirely closed or entirely open causing ambiguity in the correct choice of which isotope model to apply with mixing, also biasing $\Delta\delta^{30}$Si as described above.

In polar regions, biological production associated with seasonal sea ice adds additional complexity to silicon isotope dynamics. In the open waters of the Southern Ocean the limited data available suggest that the isotopic composition of opal sinking to depth reflects patterns in the diatom δ^{30}Si from the mixed layer (Varela et al., 2004; Fripiat et al., 2012). However, within the relatively closed sea-ice environment of the Antarctic Sea-ice Zone, sea-ice diatoms become distinctly heavy (Fripiat et al., 2007). In that study the unique isotopic signature of the sea ice flora was not detected in the bulk opal signal from the open waters; however, Varela et al. (unpublished) found a significant positive correlation

between the isotopic composition of opal and the percent ice cover in the Canadian Basin of the Arctic Ocean suggesting a significant contribution of sea ice diatoms to the isotopic signature of opal in open water. Given the importance of sea ice dynamics in polar oceans resolving the contribution of the unique sea ice flora to the silicon isotope dynamics remains an outstanding challenge.

2.4. Other pelagic biogenic opal producers

In addition to diatoms, other organisms produce biogenic opal, including heterotrophic single-celled radiolarians (supergroup Rhizeria) that live throughout the water column, choanoflagellates (family Acanthoecidae) and silicoflagellates. Considerably less work has been carried out on Si isotope fractionation by radiolarians compared to diatoms (for some discussion, see Wu et al., 1997; Egan et al., 2012; Hendry et al., in press) and, currently, nothing is known about Si fractionation by silicoflagellates or choanoflagellates.

3. Silicon isotopes in sponge spicules as a silicic acid concentration proxy

Whilst sponges are generally considered less important than diatoms to the oceanic Si budget, recent studies suggest that they may contribute more than previously thought to the global uptake of $Si(OH)_4$ (Maldonado et al., 2011). Sponges are simple filter feeding benthic animals (Animalia; Porifera), without tissue grade of organisation. Skeletal support is provided by spicules, formed from proteins, carbonate or—in the case of Classes Demospongea and Hexactinellida – opal. Sponge spicule $\delta^{30}Si$, which has a greater range and is isotopically light compared to diatoms (Egan et al., 2012), was first discussed as a potential paleoproxy a decade ago (De La Rocha, 2003). Following on from this study, two Southern Ocean calibration studies were published (Hendry et al., 2010; Wille et al., 2010), which showed the same relationship between fractionation factor (under equilibrium conditions $\varepsilon \sim \Delta\delta^{30}Si$, ranging from −1 to −5 per mil) and $Si(OH)_4$ (Hendry et al., 2011), according to Equation (3) (Hendry and Robinson, 2012):

$$\Delta\delta^{30}Si = -6.54 + \frac{270}{53 + [Si(OH)_4]} \quad (3)$$

The lack of an apparent relationship between $\delta^{30}Si$ in spicules and species or temperature, pH, salinity, etc., suggests that spicules, from different ocean basins, may provide a robust proxy for past bottom water $Si(OH)_4$ concentrations (Fig. 3; Hendry and Robinson, 2012). The non-linear relationship between $\Delta\delta^{30}Si$ and $Si(OH)_4$ concentration is likely a result of an uptake rate effect, whereby fractionation involved with uptake processes also becomes enhanced as Si uptake rates increase with concentration (Wille et al., 2010; Hendry and Robinson, 2012).

The ability of isotopes of Si to provide estimates of relative $Si(OH)_4$ depletion in surface waters (diatom $\delta^{30}Si$) together with estimates of the concentration of Si in ventilating waters (sponge $\delta^{30}Si$) makes $\delta^{30}Si$ unique among the paleo nutrient proxies. Knowing both the concentration of $Si(OH)_4$ in upwelled waters and the fraction of that Si supply that is utilized in surface waters offers the possibility of estimating absolute silica production rates in the past.

4. Challenges and caveats

4.1. Is there such a thing as a constant fractionation factor?

In order to fully understand the fractionation occurring during the biomineralization of Si, further work needs to be conducted on understanding the biochemical pathways involved in biosilicification. This is challenging as the biochemistry of biosilicification is largely unknown making it difficult to obtain a mechanistic understanding of how Si isotope fractionation arises in both diatoms and sponges. The fractionation of Si isotopes can potentially occur at several stages of the biosilicification process: uptake of $Si(OH)_4$ from seawater; polymerisation of SiO_2 within the Silica Deposition Vesicle (SDV); and efflux of excess Si from the cell. In diatoms, the efflux of Si does not impact ε (Milligan et al., 2004), which suggests that efflux does not discriminate among isotopes of Si.

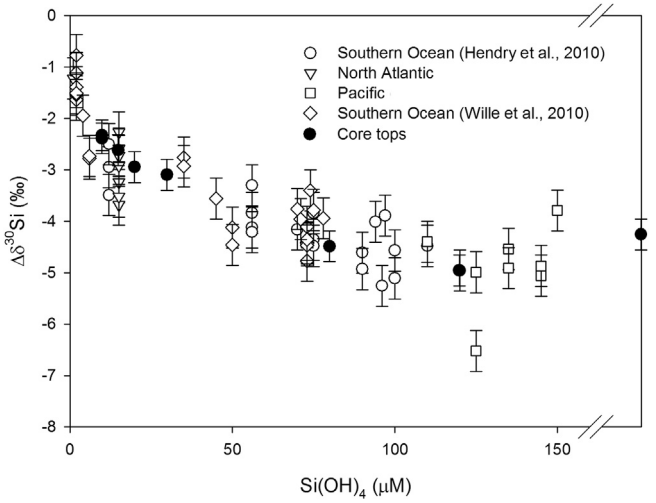

Fig. 3. $\Delta\delta^{30}Si$ for all sponges from different ocean basins. The modern sponges (open symbols) were measured without Mg doping, with error bars showing 2SD (~±0.2‰ for $\delta^{30}Si$ and 0.4‰ for $\Delta\delta^{30}Si$). The core-top spicules (solid symbols) were measured with Mg doping, with error bars showing 2SD (~±0.1‰ for $\delta^{30}Si$). Unless specified, data are from Hendry and Robinson, 2012.

The cumulative effect of these processes can be modelled for sponges assuming the fractionation occurs in several steps: firstly as the Si is transported into the cell, secondly as the Si is polymerized, and thirdly as Si is lost from the cell. The fractionation process can be expressed mathematically following Milligan et al., 2004:

$$\Delta\delta^{30}Si = \varepsilon_f = \varepsilon_{tI} + (\varepsilon_p - \varepsilon_{tE})\frac{v_E}{v_I} \quad (4)$$

where ε_f = the total Si isotopic fractionation factor, ε_{tI} = Si isotopic fractionation associated with transport into the cell, ε_p = Si isotopic fractionation associated with polymerization and ε_{tE} = Si isotopic fractionation associated with transport out of the cell; v_E = rate of Si efflux and v_I = rate of Si influx:

$$\varepsilon_f = \varepsilon_{tI} + \Delta\varepsilon_p \left\{ 1 - \frac{\frac{v_{maxp}}{\left(\frac{K_{mp}}{[Si(OH)_4]}\right)+1}}{\frac{v_{maxt}}{\left(\frac{v_{maxt}\times K_{mp}/v_{maxp}}{[Si(OH)_4]}\right)+1}} \right\} \quad (5)$$

where $\varepsilon_p = (\varepsilon_p - \varepsilon_{tE})$; K_m are the half saturation constants and v_{max} are the maximum incorporation rates. In the case of sponges, the half saturation constant and maximum incorporation rate for polymerization have been investigated in two sets of experiments and were found to be 46.41 μM and 19.33 μmol h^{-1} g^{-1} (dry weight) based on explants i.e. tissue transferred to laboratory culture (Reincke and Barthel, 1997) or 74 μM and 1.7 μmol h^{-1} g^{-1} (dry weight) based on whole specimens (Maldonado et al., 2011). The mathematical solution of Equation (5) produces non-zero values for the fractionation associated with uptake, efflux and deposition

(Hendry and Robinson, 2012). Application of a similar model to diatoms is challenging in the case of diatom field studies due to the difficulties in deconvolving apparent changes in ε due to water mass mixing (Egan et al., 2012), species variation (Sutton et al., 2013), or a possible environmental control on diatom ε as there is for sponges (Hendry and Robinson, 2012).

There have been recent developments in mixed layer modelling approaches to investigate possible mechanisms behind the apparent variation in diatom ε. Classic Rayleigh or steady state fractionation models, assuming a constant ε and a uniform upwelling water starting composition, fail to capture the range of apparent ε in the modern ocean, or the greater ε estimated from core tops (Egan et al., 2012). However, these can be reconciled in a number of ways: i) modelling uptake from waters with $\delta^{30}Si(OH)_4$ compositions that lie on mixing lines between different water masses (as discussed above, Egan et al., 2012); ii) modelling mixed layer processes that occur in the Southern Ocean to take into account higher dissolution rates relative to opal production, and greater supply of $Si(OH)_4$ relative to the uptake by diatoms (Fripiat et al., 2012).

4.2. Alteration of the production signal by fractionation during silica dissolution

One of the most significant outstanding questions in understanding the marine silicon cycle, and the role of the Southern Ocean in the distribution of $Si(OH)_4$ and silicon isotopes, is the impact of dissolution of biogenic opal on apparent isotopic fractionation as this process removes 97% of surface-produced opal leaving only 3% buried in the sediment record. There have been two published laboratory studies addressing Si isotope fractionation during opal dissolution, based on mixed-assemblage plankton trawl and sediment trap samples from the Southern Ocean (Demarest et al., 2009; Wetzel et al., 2014). The first study showed that dissolution of this material under controlled conditions preferentially released the lighter isotopes of Si with a fractionation factor of −0.55‰. This would suggest that the progressive dissolution of sinking opal would result in a trend towards increasing $\delta^{30}Si$ within opal with depth. The limited data on the isotopic composition of suspended opal with depth in the water column (e.g. Fripiat et al., 2012), and the limited core top studies of biogenic opal (Egan et al., 2012; Wetzel et al., 2014), show no indication of this trend. One hypothesis to explain this apparent discrepancy is that the dissolution of opal is not congruent among frustules with the majority of frustules found at depth or buried in sediments being relatively well preserved (note that <30% opal loss results in a non-detectable change in $\delta^{30}Si$, Demarest et al., 2009) with the remainder being nearly completely dissolved. Nelson et al. (2002) found that in the Southern Ocean the opal that survives dissolution in the upper 1000 m is nearly entirely delivered to the sea floor, consistent with the lack of changes in opal $\delta^{30}Si$ over this depth range in the Southern Ocean (Fripiat et al., 2012).

A dichotomy between frustules that completely dissolve and those that are well preserved would largely eliminate the effect of dissolution in the water column from the sediment record. However, other factors may be involved. Preliminary data on fractionation of frustules recovered from sediments show little sign of fractionation during dissolution in seawater (Beucher and Brzezinski, unpublished) suggesting the possibility of fundamental differences in the effect of dissolution on fresh (Demarest et al., 2009) and preserved opal. Other sedimentary processes such as precipitation of Si on diatom frustules (Ren et al., 2013) have yet to be explored, along with the possibility of isotopic exchange with the high concentrations of silicic acid in pore waters. It is clear that the question of the impact of dissolution and abiotic precipitation/isotope exchange on $\delta^{30}Si$ signatures must be addressed with further studies of monospecific diatom cultures and different types of biogenic silica (diatoms, sponges, radiolarians etc.) from different sources (fresh, preserved).

5. Southern Ocean influence on the modern $\delta^{30}Si(OH)_4$ distribution

Dynamics in the Southern Ocean are a major control on the distribution of $Si(OH)_4$, and its isotope composition, on a global scale. South of the SACCF (Antarctic Divergence) upwelled waters flow poleward and subduct with little biological removal of $Si(OH)_4$ resulting in the high dissolved Si concentrations of Circumpolar Deep Water (CDW) and Antarctic Bottom Water (AABW) (e.g. Marinov et al., 2006). North of the Divergence Ekman transport is equatorward and biological productivity is strong. Diatoms remove a high fraction of the dissolved Si from surface waters, then sink with a portion of frustules dissolving into the southward propagating deeper waters, returning to the Divergence as dissolved $Si(OH)_4$. This recycling loop traps $Si(OH)_4$ in the Southern Ocean water column. Frustules that escape dissolution accumulate on the sea floor forming the Southern Ocean opal belt, which – in the modern ocean – is the largest single locus of opal accumulation in the sea and is located within the Antarctic sector of the Southern Ocean to the south of the Polar Front.

Antarctic Intermediate Water (AAIW) and Sub-Antarctic Mode Water (SAMW) form by a combination of deep winter convection between the Polar Front and the Subantarctic Front (Bostock et al., 2013) and wind-driven mixing (Holte et al., 2012), forming the northward flowing shallow limb of the Meridional Ocean Circulation (MOC). AAIW and SAMW (collectively referred to as Southern Ocean Intermediate Waters, SOIW, after Pena et al., 2013) contain at least 10–15 μM silicic acid, but are depleted in $Si(OH)_4$ relative to other macronutrients (nitrate and phosphate), and it is these relatively low-silicon Mode Waters that feed into the thermocline in the lower latitudes. This can be traced by the parameter Si^*, where $Si^* = [Si(OH)_4] - [NO_3^-]$. SOIW have negative Si^* values, which can be seen far into the North Atlantic, Indian and Pacific Oceans (Sarmiento et al., 2004).

There has been recent attention paid to the role of MOC in oceanic silicon isotope distribution (de Souza et al., 2012a,b). In the high latitudes, in particular the Southern Ocean, uptake of the lighter isotopes of Si by diatoms imparts a heavy isotope signature (up to +2‰) in surface waters during the growth season, which is thought to be preserved in the winter mixed layer. The heavy isotope signature is transferred to the global thermocline via Mode Waters ($\delta^{30}Si(OH)_4 \sim +1.8‰$), and mixed into North Atlantic Deep Water (NADW, $\delta^{30}Si(OH)_4 \sim +1.6‰$) (Cardinal et al., 2005, 2007; Hendry et al., 2010; de Souza et al., 2012b). This is in contrast to deep waters in the Southern Ocean and Pacific, which have lighter $\delta^{30}Si(OH)_4$ signatures ($\delta^{30}Si(OH)_4 \sim +1.2‰$) as a result of opal remineralisation and the influence of the "production-free" signature of CDW and AABW (De La Rocha et al., 2000; Beucher et al., 2008; de Souza et al., 2012a).

5.1. Modelling global Si isotope distributions

Modelling of the global marine silicon isotope distribution requires special consideration of deep remineralisation of opal compared to organic matter, and the important role played by the Southern Ocean and, in particular, Mode Waters, which are poorly represented in many climate models. The absolute isotope values obtained in simulations are also sensitive to the $\delta^{30}Si$ of the Si entering the oceans, although the relative differences between ocean basins and water masses are robust against the isotopic value of the assumed source. Rivers are the main source of Si to the ocean

(Tréguer et al., 1995) and have an average $\delta^{30}Si$ of +0.8‰ (De La Rocha et al., 2000; Georg et al., 2009). The $\delta^{30}Si$ of river waters is mainly controlled by weathering (Ziegler et al., 2005) and could vary under large climatic or tectonic changes on timescales of 100,000 years or longer (De La Rocha and Bickle, 2005). Hydrothermal waters are another source of Si to the sea (~10% the magnitude of the river source). Few $\delta^{30}Si(OH)_4$ data from hydrothermal fluids are available; two samples collected from vents on the East Pacific Rise show negative values of −0.2 and −0.4‰ close to the average value for igneous rock −0.3‰ (De La Rocha et al., 2000).

Wischmeyer et al. (2003) published the first simulation of the global distribution of silicon isotopes in the world ocean using the Hamburg Model of the Ocean Carbon Cycle, V4. This simulation relied on the assumptions that 1) fractionation during silica production is constant with $\varepsilon_{DSi\text{-}BSi} = -1.1‰$, 2) river inputs balance permanent Si burial in sediments and 3) the dissolution of diatom frustules does not affect their isotopic composition (the study was conducted prior to the discovery of fractionation during opal dissolution). Model output showed the $\delta^{30}Si(OH)_4$ distribution in the surface waters to be inversely related to the $Si(OH)_4$ concentrations in accordance with the expectation from Rayleigh fractionation of increasing $\delta^{30}Si(OH)_4$ with greater $Si(OH)_4$ consumption. Plotting the two variables against each other revealed that their relationship was not a simple Rayleigh distillation curve as the isotopic composition of dissolved silicon not only traces its biological consumption, but also the mixing of water masses with different $\delta^{30}Si(OH)_4$ signatures (Wischmeyer et al., 2003). A puzzling result of the Wischmeyer et al. (2003) model was its failure to reproduce the observed decrease in $\delta^{30}Si(OH)_4$ between the deep Atlantic and Pacific basins (De La Rocha et al., 2000), possibly due to an excess of nutrient drawdown in the Southern Ocean due to the lack of iron limitation (Reynolds, 2009).

Multi-box models have been more successful in simulating silicon isotope distributions (De La Rocha and Bickle, 2005; Reynolds, 2009; de Souza et al., 2012b), and new generation GCMs are showing themselves to be promising with respect to reconstructing the Si cycle. Reynolds (2009) used a seven box model (Toggweiler, 1999) and the ten-box PANDORA box model (Broecker and Peng, 1987) to examine global marine silicon isotope distributions. The results of the seven box model are presented here (Fig. 4) although the results from the PANDORA model are similar. Incomplete $Si(OH)_4$ use in the surface waters of the Southern Ocean is a major driver of the model results. The dissolution of diatom frustules formed under incomplete $Si(OH)_4$ consumption impart similarly light $\delta^{30}Si(OH)_4$ values to CDW/AABW. The northward flow of Southern Ocean water masses strongly influences the isotopic composition of bottom waters in the Atlantic and Pacific basins. Outside the Southern Ocean the isotopic signature of NADW in the model is largely set by the strong ventilation in the north Atlantic.

5.1.1. Agreement and discrepancies between simulations and measurements

Comparison of the model results of Reynolds (2009) with the few measurements available from the deep Atlantic and Southern Oceans shows both agreement and significant anomalies between model predictions and data. The model predicts the observed relatively heavy $\delta^{30}Si(OH)_4$ values in NADW and lighter values in CDW (Fig. 5). The mechanisms in the model leading to this gradient are the strong biological consumption of $Si(OH)_4$ in the surface waters feeding into the well ventilated NADW combined with the effects of incomplete Si consumption in Southern Ocean surface waters mentioned above. The model was not constructed in a way to predict $\delta^{30}Si(OH)_4$ values of the deep waters of the Pacific (Figs. 4 and 5), but the PANDORA version of the model predicts a decrease

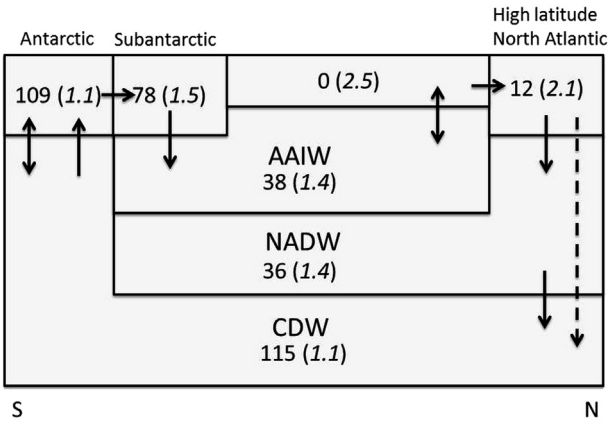

Fig. 4. Results using a seven box model simulating $Si(OH)_4$ concentrations and $\delta^{30}Si(OH)_4$ distributions (italics in parentheses). Surface boxes from left to right correspond to the Antarctic, Subantarctic, Low Latitude surface waters and the Subarctic. Adapted from Reynolds (2009). Abbreviations taken from Reynolds (2009): AAIW = Antarctic Intermediate Water (essentially Mode Waters comprising Antarctic Intermediate Waters and Subantarctic Mode Water); CDW = Circumpolar Deep Water; NADW = North Atlantic Deep Water.

in $\delta^{30}Si(OH)_4$ with increasing $[Si(OH)_4]$ along the MOC (Reynolds, 2009).

Beucher et al. (2008)'s examination of the global deep water $\delta^{30}Si(OH)_4$ data set indicates that key mechanisms are operating in the Pacific that are not captured in current models. When data from waters >2000 m in the Southern and Pacific Oceans are plotted as a function of $1/[Si(OH)_4]$ most data fall along a single straight line suggesting that a simple mixing model can explain most results (Fig. 5). The high concentration end member is the Northeast Pacific Silicic Acid Plume that originates in the Cascadia Basin (Johnson et al., 2006) that has $[Si(OH)_4]$ >150 μM corresponding to a $1/[Si(OH)_4]$ value of ~0.005 in Fig. 5. The other end member lies in the Southern Ocean. In contrast, the data from the North Pacific and the Northwest Pacific fall on a trajectory of decreasing $\delta^{30}Si(OH)_4$ with increasing $[Si(OH)_4]$ from the Atlantic to the Southern Ocean and Pacific as predicted by models (Reynolds, 2009).

A hypothesis that explains the anomalous isotope patterns in the Pacific is that the Northeast Pacific $Si(OH)_4$ Plume (Johnson et al., 2006) exerts a major influence on Si isotopes in this region. The flux of $Si(OH)_4$ from the sediments beneath the Plume is large (1.5 Tmol Si a^{-1}) equivalent to a third of that supplied to the global ocean by rivers (Johnson et al., 2006). Its influence extends to the west and to the south, but apparently not as far west as the stations in the North Pacific (23°N, 158°W, De La Rocha et al., 2000) and NW Pacific (24.3°N, 170.3°W) presented in Fig. 5. This feature has not been incorporated into models of Si isotope distributions. Note that the $\delta^{30}Si(OH)_4$ of the waters in the Plume, +1.4‰, is much more positive than hydrothermal sources (~−0.3‰, De La Rocha et al., 2000) suggesting a biogenic source. The $\delta^{30}Si(OH)_4$ of the Plume is similar to that in the North Atlantic (Fig. 5) so that it's influence essentially eliminates contrasts in $\delta^{30}Si(OH)_4$ between the deep Atlantic and deep Northeast Pacific.

The main point to be taken from this analysis is that the spatial resolution of the present $\delta^{30}Si(OH)_4$ data set is inadequate to evaluate mechanisms leading to even the first-order distribution of isotopes of Si in the global ocean although strong anomalies point to possible explanations. The level of variability in $\delta^{30}Si(OH)_4$ within Pacific deep waters far exceeds that predicted by current models and trends between Si isotopes and Si concentration are opposite of model predictions, possibly due the Northeast Pacific Silicic Acid Plume, but other unanticipated mechanisms may be involved. New data from the International GEOTRACES program

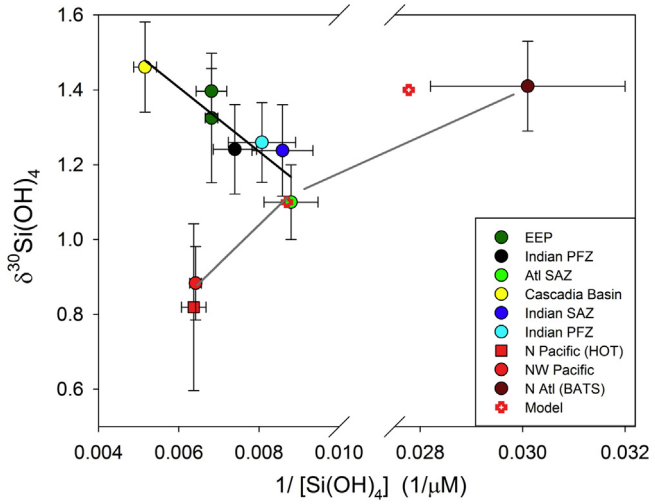

Fig. 5. $\delta^{30}Si$ versus $1/[Si(OH)_4]$ for waters below 2000 m (adapted from Beucher et al., 2008). EEP, Eastern equatorial Pacific; AZ, Antarctic Zone; SAZ, Subantarctic Zone; PFZ, Polar Frontal Zone; HOTS, Hawaiian Oceanic Time Series; BaTS, Bermuda Time Series. Linear regression of data from Southern Ocean and Eastern Pacific. Grey line drawn by eye. Model results from Reynolds (2009).

that is producing sections of $\delta^{30}Si(OH)_4$ distributions along several major ocean sections should help resolve these issues.

6. Paleoceanographic applications and multi-proxy approaches

In addition to the whole-ocean concentration, biogenic opal production is controlled by the distribution of $Si(OH)_4$ in the global ocean. Since their evolution, diatoms have dominated the marine silicon cycle and opal formation, such that they have effectively stripped $Si(OH)_4$ out of surface waters (Falkowski et al., 2004), resulting in pervasive Si limitation of silica production (or co-limitation with other nutrients e.g. iron) in low latitude regions (e.g. Brzezinski and Nelson, 1996; Brzezinski et al., 2008). Net diatom production relies on upwelled sources of dissolved silicon; changes in ocean circulation and upwelling are therefore key to controlling opal production and carbon drawdown by diatoms.

Particular hypotheses that have received attention over the last decade are the Silicic Acid Leakage Hypothesis (SALH; Brzezinski et al., 2002; Matsumoto et al., 2002) and the related silica hypothesis (Harrison, 2000; Nozaki and Yamamoto, 2001). The silica hypothesis states that diatom productivity was promoted during glacials as a result of an increase in Si supplied from dust, contributing to the drawdown of CO_2 (Harrison, 2000). In contrast, the SALH posits that, during Pleistocene glacials, the addition of iron via enhanced dust deposition in the Southern Ocean results in a change in diatom physiology, such that diatoms take up macronutrients at a lower Si:N ratio. This arises from the combination of decreased cellular N content in most, if not all diatoms, and the thickening or thinning of the siliceous frustules in response to low Fe (Hutchins et al., 1998; Takeda, 1998; Marchetti and Harrison, 2007). Even in cases where diatoms thin their frustules in response to low Fe (Marchetti and Harrison, 2007) the reduction in cellular N is even greater such that increased Si:N is a universal response. The addition of Fe to modern day Southern Ocean waters shifts Si:N uptake ratio from a value of 4–8 under ambient conditions to a value of 2 (Frank et al., 2000). Given the $[Si(OH)_4]:[NO_3^-]$ ratio of ~2.3 in upwelling waters at the Antarctic Divergence, release from Fe stress during glacial times would cause approximately half of the upwelled silicic acid to remain in surface waters upon nitrate depletion (Brzezinski et al., 2002). The net result is that the water which subducts to form the all-important SOIW that ultimately feed the lower latitude thermocline, would have both higher $[Si(OH)_4]$ and a higher Si:N ratio. Ventilation of the relatively Si-rich SOIW at low latitude would promote the growth of diatoms relative to carbonate producers, altering the $C_{org}/CaCO_3$ rain ratio and ocean alkalinity to lower atmospheric CO_2 (Rickaby et al., 2007; Matsumoto and Sarmiento, 2008). Opal-based silicon isotope proxies are ideal tools for investigating the SALH, and to investigate other past changes in the marine silicon cycle (Fig. 6).

6.1. Silicic acid leakage from the Southern Ocean

6.1.1. Opal mass accumulation rates and $^{231}Pa/^{230}Th$

For the SALH to be accepted, there has to be evidence for a change in Si utilization in the Southern Ocean, which would have provided the excess $Si(OH)_4$ to escape to lower latitudes. Records of Southern Ocean opal mass accumulation rates (MAR) since the Last Glacial Maximum (LGM) provide a consensus view that the main belt of opal deposition around Antarctica shifted northwards compared to today, into the subantarctic zone (reviewed by Bradtmiller et al., 2009). These records also imply that there was no net increase in opal production that could have contributed to a drawdown of atmospheric pCO_2 in either the Atlantic or Indian Sectors of the Southern Ocean (Kumar et al., 1995; Frank et al., 2000). However, there was a decrease during the LGM of total mass flux in the Pacific Sector, which is the main candidate for potential leakage of $Si(OH)_4$ to the lower latitudes (Chase et al., 2003a; Bradtmiller et al., 2009).

6.1.2. Opal isotope proxies

Si isotope records. Glacial-interglacial changes in Si utilization by diatoms south of the modern Antarctic Polar Front was the first paleoclimate question to be addressed using the diatom opal $\delta^{30}Si$ proxy (De La Rocha et al., 1998). These first diatom $\delta^{30}Si$ records showed that there was a lower Si utilization south of the Antarctic Polar Front at the LGM compared to today, and this finding has also been mirrored in sediment cores from the subantarctic (Beucher et al., 2007), supporting the SALH. A reduction in utilization is consistent with a decline in Si uptake by diatoms, relative to other nutrients, as a result of the alleviation of Fe stress. However, changes in dissolution and water column recycling processes, as a result of the alteration of the recirculation that produces the modern silicon trap, could also be responsible for the observed shifts in diatom $\delta^{30}Si$.

Si–N isotope records. The preferential and variable uptake of $Si(OH)_4$ over NO_3 in the low-iron waters of the Southern Ocean seawater results in a decoupling of the dynamics of these two macronutrients and the preferential depletion of $Si(OH)_4$ over NO_3 in the modern Southern Ocean (Pondaven et al., 2000). The relative utilization of the two nutrients has been constrained over time using combined Si and N isotope records from diatom opal and opal-bound organic matter respectively. One of the principal aims to date has been to investigate changes in Si:N uptake rates in the Southern Ocean over glacial-interglacial timescales as a test of the SALH (Robinson et al., 2005b; Beucher et al., 2007; Crosta et al., 2007; Horn et al., 2011). Although there are analytical challenges surrounding the robust application of diatom-bound N isotopes (Robinson et al., 2004), these studies generally agree that there was relatively higher utilization of N in surface waters compared to $Si(OH)_4$ during the Last Glacial Maximum, suggesting a relatively high Si:N ratio in Mode Waters, and supporting the SALH (e.g. Horn et al., 2011). More recent studies are beginning to delve into $Si(OH)_4$ leakage deeper in time, such as an investigation of the role of southern sourced water in driving the highly productive Matuyama

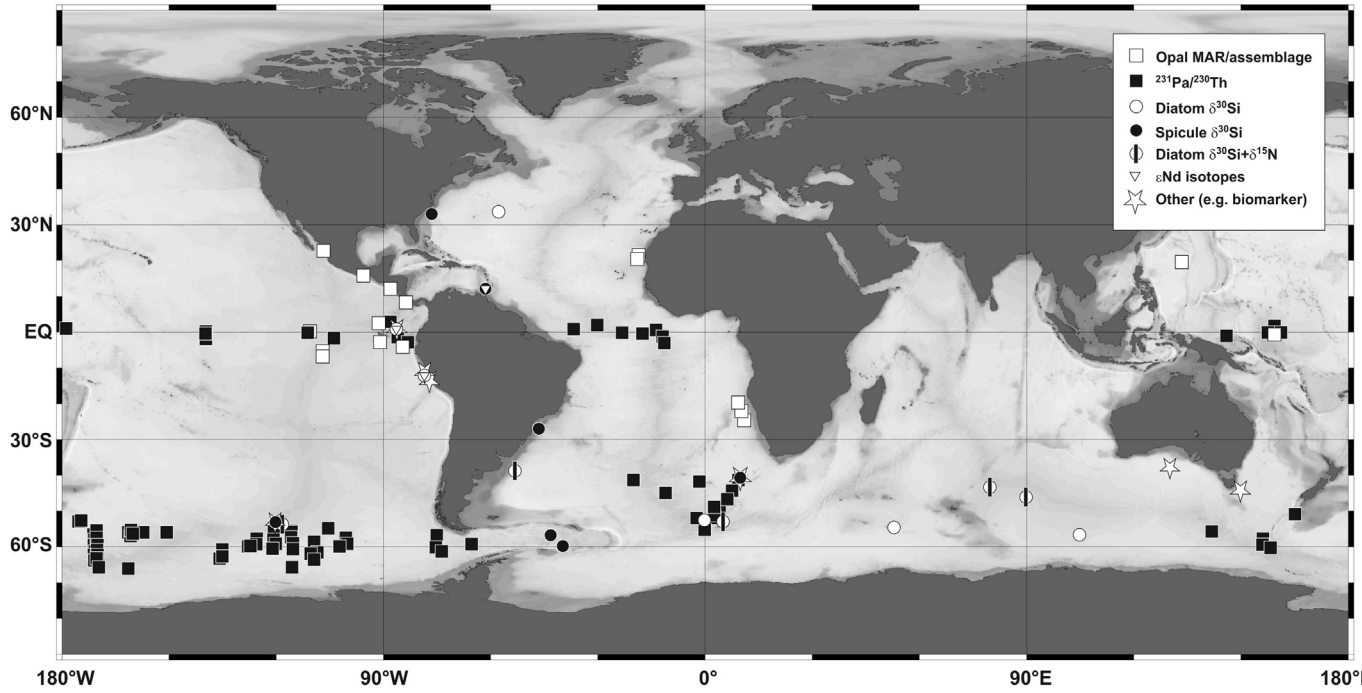

Fig. 6. Map showing location of studies specifically aimed at investigating the SALH. Drawn using Ocean Data View (Kumar et al., 1995; De La Rocha et al., 1998; Frank et al., 2000; Chase et al., 2003a; Calvo et al., 2004; Higginson and Altabet, 2004; Pichat et al., 2004; Robinson et al., 2005b; Bradtmiller et al., 2006, 2007, 2009; Kienast et al., 2006; Beucher et al., 2007; Crosta et al., 2007; Richaud et al., 2007; Pichevin et al., 2009; Zhai et al., 2009; Dubois et al., 2010; Ellwood et al., 2010; Hendry et al., 2010; Pichevin et al., 2010; Romero, 2010; Arellano-Torres et al., 2011; Calvo et al., 2011; Hayes et al., 2011; Horn et al., 2011; Romero et al., 2011; dos Santos et al., 2012; Hendry et al., 2012; Ehlert et al., 2013; Meckler et al., 2013; Pena et al., 2013; Hendry et al., in press).

Diatom Maximum in the Benguela Upwelling System (Ocean Drilling Program Site 1082, 21.1°S, 11.8°E, 1279 m water depth) from 2 to 3 Ma (Etourneau et al., 2012). The heaviest diatom $\delta^{30}Si$ signal corresponded with the highest opal accumulation rate, and the lightest diatom-bound $\delta^{15}N$, which could be explained by the growth of mat-forming diatoms due to an increased $Si(OH)_4$ supply from southern sourced water, but weak upwelling. The mat-forming diatoms efficiently utilised a large proportion of the available Si, resulting in Si-limitation of surface waters and relatively low N utilization (Etourneau et al., 2012).

Paired diatom-sponge Si isotopes. In an analogous fashion to paired benthic-planktonic foraminifera carbon isotopes, paired sponge-diatom silicon isotope records can be used to quantify the marine silicon cycle of the whole water column: the supply of dissolved $Si(OH)_4$ from deep waters, and the utilization of silicon in surface waters by diatoms in the Southern Ocean. To date, the multi-proxy approach has been used to investigate the SALH since the Last Glacial Maximum (Hendry et al., 2010, 2012; Horn et al., 2011). These studies have been able to constrain deep water $Si(OH)_4$ concentrations (Hendry et al., 2010) and the upwelling rate of $Si(OH)_4$ (Horn et al., 2011). The records show a dramatic increase in upwelling supply, confirmed an increase in the utilization of Si (Horn et al., 2011), and a slight transient decrease in the concentration of $Si(OH)_4$ in deep waters across the Last Glacial termination (Hendry et al., 2010).

Paired Si–Ge records. One important caveat that needs to be considered when reconstructing $[Si(OH)_4]$ from sponge spicule $\delta^{30}Si$ using Equation (5) is that the isotopic composition of the $Si(OH)_4$ is required to calculate $\Delta\delta^{30}Si$. Thus the estimated $Si(OH)_4$ concentration is a function of the measured spicule $\delta^{30}Si$ and for paleo – reconstructions, the assumed deep water $\delta^{30}Si(OH)_4$. As discussed above deep water $\delta^{30}Si(OH)_4$ is tied to water mass distributions within the MOC in the modern. Deviations from the modern in the past will depend both on i) the secular shift in whole ocean $\delta^{30}Si$ through time, on timescales greater than the residence time of Si in the global oceans ($\sim$10 ka, Georg et al., 2009; Tréguer and De la Rocha, 2013), for example due to changes in subglacial weathering processes and meltwater inputs to the ocean (Opfergelt et al., 2013); and ii) on changes in the distribution of silicon isotopes in the oceans resulting from ocean circulation changes, on timescales of thousands of years or more.

Previous studies have taken these changes into account through simple modelling efforts (e.g. Hendry et al., 2012; Griffiths et al., 2013) or by pairing with diatom $\delta^{30}Si$ (Egan et al., 2012). However, an alternative approach is to use, in addition to spicule $\delta^{30}Si$, sponge and diatom Ge/Si ratios. Spicule Ge/Si will record not only secular changes in seawater Ge/Si, which can be corrected for using diatom Ge/Si (thought to be a recorder of secular changes in whole ocean Ge/Si, although there needs to be a more thorough assessment of vital effects (Froelich et al., 1992), but also a component of $Si(OH)_4$ concentration. In other words, spicule $\delta^{30}Si$ and Ge/Si provide complementary access to past ocean $Si(OH)_4$ concentrations. This approach has been used to investigate the SALH: Ge/Si and Si isotope proxies in sediment cores from the Atlantic and Pacific Sectors ($\sim$41°S, $\sim$10°E, 4600 m water depth, and $\sim$53°S, $\sim$120°W, 2700 m water depth) of the Southern Ocean show that there was a build-up of nutrients during glacial periods in the Pacific Sector only, consistent with opal accumulation records (Chase et al., 2003a; Bradtmiller et al., 2009; Ellwood et al., 2010).

6.2. Impact of silica leakage on the low latitudes

6.2.1. Opal accumulation rates

Records of opal mean accumulation rate (MAR), ^{230}Th-normalised opal MAR, and downcore $^{231}Pa/^{230}Th$ do not reveal a clear picture of changes in low latitude diatom productivity over glacial-

interglacial and millennial timescales in response to $Si(OH)_4$ leakage, pointing towards multiple controls in Si supply and uptake. In the Central and Eastern Equatorial Pacific, and the Peru upwelling zone, ^{230}Th-normalised opal fluxes are higher at Marine Isotope Stage (MIS) 3 (~30–60 ka) than during MIS2 (~20–30 ka), with either similar or lower opal fluxes during the Last Glacial Maximum compared to the Holocene, which is inconsistent with the SALH (Bradtmiller et al., 2006; Kienast et al., 2006; Richaud et al., 2007). However, records going back further into the Pleistocene show higher ^{230}Th-normalised opal fluxes at the glacial terminations than at full glacial conditions or during interglacials, but these peaks are not observed for all terminations, and there are peaks in opal flux not associated with terminations (Bradtmiller et al., 2006; Dubois et al., 2010; Hayes et al., 2011). In contrast, the Eastern Tropical North Pacific (ETNP) shows higher opal MAR at the glacials compared to the interglacials (Arellano-Torres et al., 2011). In the Western Pacific, large diatom mats in the Phillipines Sea, comprising *Ethmodiscus rex*, have been carbon dated to MIS2 (Zhai et al., 2009). However, ^{231}Pa/^{230}Th and ^{230}Th-normalised opal fluxes from another core in the Western Equatorial Pacific indicates lower productivity in glacial periods (Pichat et al., 2004).

Similar inconsistencies occur in the Atlantic. In the Equatorial Atlantic, the sediment cores that have been analyzed to date show higher opal accumulation and corresponding ^{231}Pa/^{230}Th during the Last Glacial, with peaks occurring at the deglaciation, although these cores do not have sufficient sedimentation rates to resolve fully Heinrich Stadials, the abrupt climate events of the Lateglacial and deglacial (Bradtmiller et al., 2007). Other sites in the Eastern North Atlantic show clearer abrupt increases in opal export during the deglacial, which correspond with oceanic and/or atmospheric reorganisation during the Heinrich Stadials (Romero et al., 2008; Meckler et al., 2013).

In addition to inherent preservation bias, there are a number of reasons why the low latitude opal accumulation rate records need to be treated carefully in the context of the SALH. Firstly, the opal MAR records reveal complex temporal and spatial patterns, reflecting a number of regional and local controls on productivity. Secondly, tropical opal burial reconstructions cannot distinguish between the silica hypothesis of Harrison (2000) and the SALH *senso stricto* (Brzezinski et al., 2002) i.e. opal records cannot provide a mechanistic interpretation for productivity changes. Thirdly, $Si(OH)_4$ leakage may not manifest in an increase in opal accumulation rate, *per se*, but an increase in the productivity of opal-producers relative to carbonate producers, and still produce a shift in ocean alkalinity and pCO_2 drawdown (Matsumoto and Sarmiento, 2008). In other words, the lack of a coherent change in low latitude opal accumulation rates is not sufficient to reject the SALH. Instead, a multi-proxy approach allows the various interacting controls on productivity to be deconvolved, and specific hypotheses regarding the SALH to be tested.

6.2.2. Multi-proxy isotope records of low latitude changes in water mass and ecology

Sponge spicule silicon isotopes. An important concept that follows from the SALH is that intermediate waters subducting away from the Southern Ocean must have increased in $Si(OH)_4$ during the glacial. Sponge spicule δ^{30}Si records of benthic $Si(OH)_4$ concentrations provides one of the most direct methods for testing this assertion. Spicule isotopic records from core site GeoB2107-3 (27°S, 46°W, 1050 m water depth), which is bathed in modern AAIW, show that the $Si(OH)_4$ concentrations were not significantly different at the LGM compared to today. However, the records show pulses of heavy δ^{30}Si – indicative of high $Si(OH)_4$ concentrations – during the abrupt events of the Lateglacial and deglacial, Heinrich Stadials (HS) One and Two, and the Younger Dryas (Hendry et al., 2012). In other words, leakage of high Si waters from the Southern Ocean to lower latitudes occurs, but during abrupt climate change events rather than on glacial-interglacial timescales.

Paired Si–Nd isotopes. Due to biogeographical variations and ocean circulation, Southern Ocean deep waters are characteristically $Si(OH)_4$ – rich, and changes in their $Si(OH)_4$ content can be traced by the δ^{30}Si of benthic sponge spicules (Hendry et al., 2010). The Nd isotope composition (εNd) of bottom water, recorded in fish teeth, sediments, and Fe–Mn coatings of planktonic foraminifera in some oceanographic settings (e.g. Pahnke et al., 2008; Piotrowski et al., 2008; Roberts et al., 2010), provides an additional method of "labelling" southern sourced waters, due to a distinctive radiogenic signature from mixing with Pacific waters (Albarede et al., 1997). However, one key problem with the εNd proxy is that the Nd southern and northern end members could change over relevant timescales (Pahnke et al., 2008). The part of the water column that is represented by planktonic foraminiferal coatings is also apparently variable (Roberts et al., 2010; Pena et al., 2013). A combination of these benthic δ^{30}Si and εNd can, however, provide a more robust means of tracing southern sourced water.

To date, this has been used to investigate the SALH across MIS4 (~60–70 ka) in the tropical Atlantic (Griffiths et al., 2013), and more localised processes in the Peruvian upwelling zone of the South Pacific (Ehlert et al., 2013). Of relevance to the SALH, Griffiths et al. (2013) found that both "tracers" indicated an increase in the presence of southern component water in a sediment core off the coast of Brazil (core site MD99-2198, 12.09°N; 61.23°W; 1330 m water depth) across the MIS 5/4 boundary, consistent with a modest leakage of relatively Si-enriched water from the Southern Ocean at this time via SOIW. However, further work is required to understand the relationship between these two proxies, given the slight differences in the timing and nature of the changes recorded in core MD99-2198.

Si–N isotopes. Diatom Si and diatom-bound N isotopes from a core in the Eastern Equatorial Pacific support a reduction in Si uptake relative to other nutrients due to the alleviation of Fe stress – and limitation by Si and N – during the glacial. The authors argue for a fundamental change in nutrient limitation in the region, with a likely glacial switch to phosphorus limitation away from Si–Fe co-limitation (Pichevin et al., 2009).

7. Silicic acid leakage form the Southern Ocean – new insights and changing perspectives

The SALH has been tested repeatedly over the past few years. One of the key issues, and the main defining difference between the silica hypothesis (Harrison, 2000) and the SALH *senso stricto* (Brzezinski et al., 2002), is the extent to which SOIW distributions have changed over glacial-interglacial and millennial timescales. Other geochemical archives have been used to investigate changes in intermediate water formation and distribution, including stable carbon isotopes (Spero and Lea, 2002; Bostock et al., 2004; Pahnke and Zahn, 2005; Bostock et al., 2010), diatom-bound carbon isotopes (Xiong et al., 2013), radiocarbon (Keigwin, 2004; Robinson et al., 2005a; Mangini et al., 2010; Burke and Robinson, 2011; Thornalley et al., 2011), εNd (Pahnke et al., 2008; Xie et al., 2012; Pena et al., 2013), and biomarkers (Calvo et al., 2004, 2011; Higginson and Altabet, 2004; dos Santos et al., 2012). Some coherent pictures have begun to arise of expanded AAIW during glacials, especially in the Pacific (Bostock et al., 2004, 2010), with intense deep mixing with CDW and Glacial Antarctic Bottom Water (GAABW), expanded oligotrophic surface waters in the Subantarctic and so a strong subsurface nutrient gradient (Bostock et al., 2004,

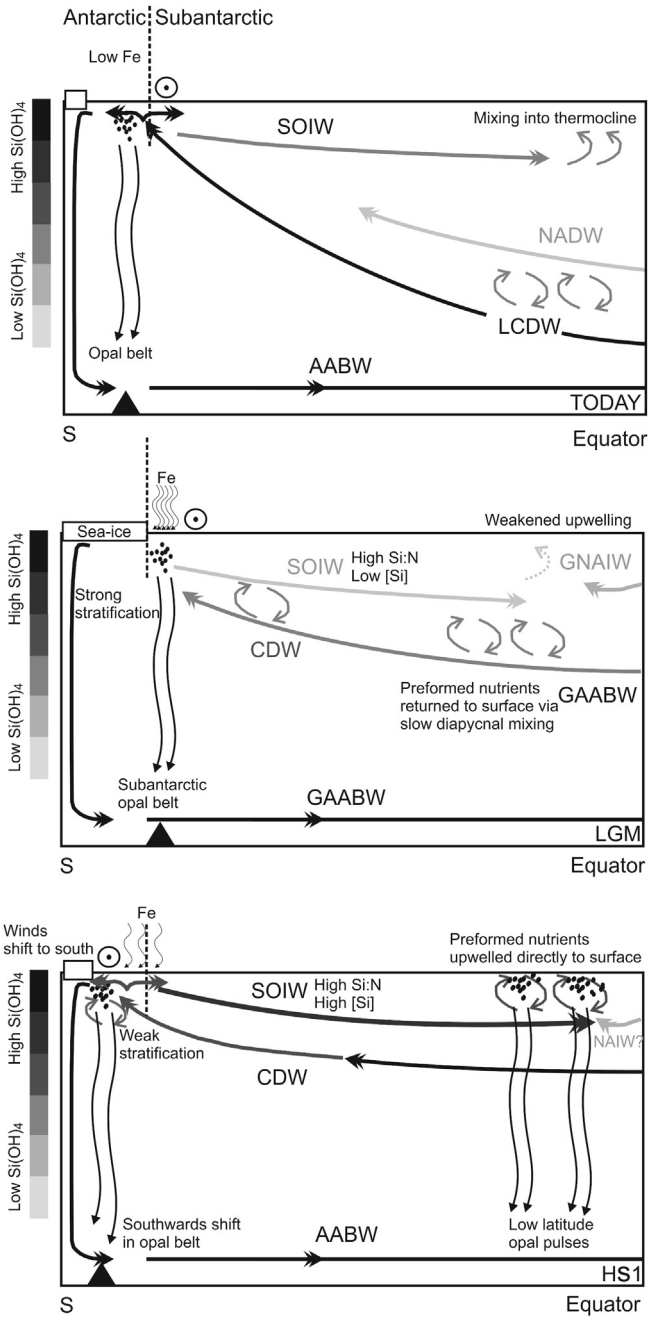

Fig. 7. Cartoon illustrating the **"Silicic Acid Ventilation Hypothesis" (SAVH)**. LCDW = Lower Circumpolar Deep Water; GNAIW = Glacial North Atlantic Intermediate Water; GAABW = Glacial Antarctic Bottom Water; SOIW = Southern Ocean Intermediate Water. The black triangle shows the location of the Southern Ocean opal belt. During the LGM, Mode Waters formed with a high Si:N ratio, due to changes in utilization and dissolution processes resulting from Fe fertilization and a northwards movement of the opal belt (Bradtmiller et al., 2009). Buoyancy-driven stratification in the Southern Ocean and weaker mixing in the Subantarctic, coupled with weaker upwelling in key regions (e.g. Benguela Upwelling System, (Romero, 2010)) increases the ratio of Si:N in SOIW, but reduces the concentration of Si, and so reduces the supply of Si to low-latitude thermocline waters. At Heinrich Stadial 1 (HS1, 16–18 ka), ice-rafting in the North Atlantic drives a collapse of GNAIW (McManus et al., 2004), a southwards shift of the Atlantic Intertropical Convergence Zone (ITCZ), a strengthening of the NE Trade Winds (Vink et al., 2001) and a southwards shift in the Southern Ocean Westerlies (Anderson et al., 2009). These atmospheric changes could have resulted in stronger upwelling in some regions of the North Atlantic and Pacific Oceans (Koutavas and Sachs, 2008; McClymont et al., 2012). Enhanced wind-driven upwelling, and greater mixing in the Subantarctic, together with a breakdown of buoyancy-driven stratification in the Southern Ocean, would have led to high Si:N and high Si concentration SOIW. A concurrent increase in ventilation in the Southern Ocean and the 2010). Furthermore, carbon isotopes suggest widespread pulses of well-ventilated SOIW formation during the Heinrich Stadials and Younger Dryas (Pahnke and Zahn, 2005).

Other lines of evidence point towards expanded SOIW during abrupt climate events of the deglacial e.g. Nd isotope record from the Tobago Basin and East Equatorial Pacific (Pahnke et al., 2008; Pena et al., 2013). Another εNd record from the Florida Straits points towards reduced SOIW presence in the North Atlantic during Heinrich Stadial One and the Younger Dryas (Xie et al., 2012). However, this study assumed almost pure AAIW filled the study site basin, an assumption that is not supported by modern hydrographic data (Pena et al., 2013). These disagreements highlight the complex nature of reconstructing oceanic circulation, and the problems with geochemical proxies, for example in terms of signal redistribution (Gutjahr et al., 2008) and changing water mass end-members (Pahnke et al., 2008).

The opal-based evidence from the Southern Ocean discussed above, combining opal δ^{30}Si records with other palaeoproxies, indicates that there were major ecological changes in the Southern Ocean over glacial-interglacial timescales, which would have led to a change in the composition of SOIW. The Si:N ratio would increase during glacials either due to a change in i) utilization of Si relative to N as a result of Fe fertilization (Brzezinski et al., 2002), or ii) the location of the opal belt such that dissolution and regeneration of opal occurs in the region of SOIW subduction (Bradtmiller et al., 2007). However, proxy evidence from low latitudes suggests that, on glacial-interglacial timescales, the impact on lower latitude ecology, and climate, was minimal. A reduction in the rate of SOIW supply, or indeed a change in the depths to which the subducted waters penetrated, over glacial-interglacial timescales may have limited the extent to which the southern sourced preformed nutrients could upwell in the low latitudes (Crosta et al., 2007). Rather, it was changes on abrupt (millennial) timescales in ocean circulation and wind-driven upwelling (Moreno et al., 2002; Anderson et al., 2009) during glacial terminations that enhanced the supply of – most likely – southern sourced Si-rich water that drove the major ecological changes observed in lower latitude sedimentary cores (Bradtmiller et al., 2009; Pahnke et al., 2008; Calvo et al., 2011; Hendry et al., 2012). The most-cited sources for these southern-component waters are SOIW (e.g. Pahnke et al., 2008; Calvo et al., 2011; Pena et al., 2012; Hendry et al., 2012), which are known to feed the lower thermocline with nutrients in the low latitudes (Sarmiento et al., 2004). However, it has also been speculated that the $Si(OH)_4$ feeding the low latitude peaks in opal production seen in the Equatorial and North Atlantic originated from upwelling deep southern component water through a large-scale change in ocean circulation (Meckler et al., 2013). However, the similarity of the deglacial opal peaks in the low-latitude Atlantic and Pacific Oceans (Bradtmiller et al., 2006, 2007) would require a process that could operate in both basins despite the different deep-water mass configurations, and so could be used to argue against a deep southern component water mechanism.

Could changing nutrient dynamics in the Southern Ocean alter southern-sourced Mode Waters to cause major changes in nutrient distribution during abrupt climate change? Whilst a speculative twist on the SALH, such events may be the logical outcome of the shifts in Southern Ocean circulation and nutrient supply during glacial terminations. Glacial periods are characterized by the northward shift in the westerly winds in the Antarctic coupled with strong stratification south of the Polar Front due to buoyancy-

low-latitudes would have led both to an export of these high Si:N and high [Si] waters and an increase in their supply to thermocline and surface waters, promoting low-latitude diatom production.

forcing and reduced wind-stress (Marshall and Speer, 2012). Diatom productivity and the opal belt also shifted northward supported mainly by upwelling within the Subantarctic (Bostock et al., 2004; Beucher et al., 2007). Upwelling and mixing to the north of the Polar Front in the Subantarctic would not be as efficient in tapping high-nutrient deeper waters compared to the circulation associated with the Antarctic Divergence, diminishing nutrient supply during glacials. The northward shift in the opal belt may have been coupled with a reduction in residual silicic acid concentrations as a result of a lower supply of Si to the Subantarctic surface waters and significant diatom production. Combined with high atmospheric Fe supply this would result in SOIW with high Si:N ratio, but diminished Si concentrations. Hence, SOIW mixing with low-latitude thermocline waters did not promote significant diatom growth, especially in regions where wind-driven upwelling was also weakened during glacial times (e.g. Moreno et al., 2002).

However, during HS1, sustained Fe supply to the Southern Ocean, continued mixing in the Subantarctic (e.g. Bostock et al., 2004), together with a breakdown of stratification and increased upwelling in the Antarctic (e.g. Anderson et al., 2009; Burke and Robinson, 2011) would re-establish the Antarctic Divergence and – once again – lead to the efficient tapping of deeper waters. Such an increase in upwelling would result in an increase in both Si and oceanic Fe supply to surface waters (Ayers and Strutton, 2013), despite reducing atmospheric Fe input (Lambert et al., 2008). Strong wind-driven mixing would result in deep winter convection (Holte et al., 2012) and formation of SOIW with high Si concentrations and high Si:N. At the same time, enhanced wind-driven upwelling in the lower latitudes increased the supply of these waters to the thermocline and so supported enhanced diatom growth. Whilst the atmospheric Fe supply to the surface of the Southern Ocean had declined by the Younger Dryas (Lambert et al., 2008), and the Southern Ocean Si trap was re-established, low-latitude diatom pulses still occurred in places of enhanced wind-driven upwelling as a response to enhanced mixing of oceanic Fe in the Subantarctic and changes in the vertical structure of SOIW (Hendry et al., 2012).

Key to this scenario is the change in the efficiency with which Southern Ocean circulation brings abyssal waters with high nutrients to the surface where opal formation occurs. During the glacials, that efficiency is low due to increased stratification and reduced mixing in Antarctic waters coupled with the northwards shift in the opal belt from the Antarctic Divergence to the Subantarctic, where entrainment of high-nutrient abyssal water is less pronounced. A southwards shift in the opal belt and enhanced upwelling and mixing in the Antarctic Divergence during Heinrich Stadials would increase the efficiency of oceanic nutrient supply from deep waters, and both the Si content and Si:N ratio of mode waters (Ayers and Strutton, 2013). Together these factors form the basis of a **"Silicic Acid Ventilation Hypothesis" (SAVH)** (Fig. 7) where the change in oceanic and atmospheric circulation that occurred during the Heinrich Stadials would lead both to the ventilation of waters near the Antarctic Divergence, resulting in Si-enriched SOIW, and the low-latitudes, leading to the supply of these high Si waters to the surface and triggering the widespread and abrupt ecological changes that are observed. Further investigation into intermediate depth water composition, using high-resolution records of diatom and spicule $\delta^{30}Si$, in addition to the other proxies discussed above, will be able to test the plausibility of such a mechanism.

The original SALH proposed that Si leakage during glacial times contributed to global cooling by lowering atmospheric pCO_2 during glacial periods. The more recent evidence that Si leakage from the Southern Ocean occurred predominately during deglaciations has profound implications for the effect of this mechanism on climate. Si leakage during deglaciations would drive low latitude flora towards diatoms when atmospheric pCO_2 levels were rising. This suggests that the ecological effects that would favour a decline in atmospheric pCO_2 were overwhelmed by other, possibly physical processes, such as the increased evasion of CO_2 from the ocean due to increased upwelling at the Antarctic Divergence (Anderson et al., 2009).

8. Synthesis and conclusions

The Southern Ocean plays a key role in the climate system, through heat and nutrient transfer to the global oceans. The "biogeochemical divide" formed by the Antarctic Divergence, and the formation of Mode Waters, essentially sets the global levels of preformed nutrients and stored carbon (Sarmiento et al., 2004; Marinov et al., 2006, 2008; Sigman et al., 2010). Understanding Mode Water nutrients, and how they have changed in the past, is essential for understanding past changes in both Southern Ocean and low latitude biological productivity. Diatoms dominate the phytoplankton communities in most regions of the Southern Ocean, and they impart distinctive $Si(OH)_4$ concentrations and isotope signatures on the subducting waters that form the Mode Waters. The established relationship between isotopes of Si and the MOC allows the proxy to be used as both a nutrient proxy and an indicator of water mass changes. Furthermore, biogenic opal provides an important archive of past ocean biological productivity and environmental conditions in the Southern Ocean and beyond. In particular, when used in conjunction with other sedimentary proxies, biogenic opal $\delta^{30}Si$ has shown itself to have great potential in deconvolving past signals of climatic, biogeochemical and ecological change.

Acknowledgements

KH is funded by the Royal Society, the Climate Change Consortium of Wales, the Natural Environment Research Council, and the Leverhulme Trust. MB is funded by the US National Science Foundation.

References

Albarede, F., Goldstein, S.L., Dautel, D., 1997. The neodymium isotopic composition of manganese nodules from the Southern and Indian Oceans, the global oceanic neodymium budget, and their bearing on deep ocean circulation. Geochim. Cosmochim. Acta 61 (6), 1277–1291.

Andersen, M.B., Vance, D., Archer, C., Anderson, R.F., Ellwood, M.J., Allen, C.S., 2011. The Zn abundance and isotopic composition of diatom frustrules, a proxy for Zn availability in ocean surface seawater. Earth Planet. Sci. Lett. 301, 137–145.

Anderson, R.F., Ali, S., Bradtmiller, L.I., Nielsen, S.H.H., Fleisher, M.Q., Anderson, B.E., Burckle, L.H., 2009. Wind-driven upwelling in the Southern Ocean and the deglacial rise in atmospheric CO_2. Science 323, 1443–1448.

Arellano-Torres, E., Pichevin, L.E., Ganeshram, R.S., 2011. High-resolution opal records from the eastern tropical Pacific provide evidence for silicic acid leakage from HNLC regions during glacial periods. Quat. Sci. Rev. 30 (9–10), 1112–1121.

Ayers, J.M., Strutton, P.G., 2013. Nutrient variability in subantarctic mode waters forced by the southern annular mode and ENSO. Geophys. Res. Lett. 40, 3419–3423.

Beucher, C.P., Brzezinski, M.A., Crosta, X., 2007. Silicic acid dynamics in the glacial sub-Antarctic: implications for the silicic acid leakage hypothesis. Glob. Biogeochem. Cycles 21. http://dx.doi.org/10.1029/2006GB002746.

Beucher, C.P., Brzezinski, M.A., Jones, J.L., 2008. Sources and biological fractionation of silicon isotopes in the Eastern Equatorial Pacific. Geochim. Cosmochim. Acta 72, 3063–3073.

Bostock, H.C., Opdyke, B.N., Gagan, M.K., Fitfield, L.K., 2004. Carbon isotope evidence for changes in Antarctic Intermediate Water circulation and ocean ventilation in the southwest Pacific during the last deglaciation. Paleoceanography 19. http://dx.doi.org/10.1029/2004PA001047.

Bostock, H.C., Opdyke, B.N., Williams, M.J.M., 2010. Characterising th intermediate depth waters f the Pacific Ocean using $\delta^{13}C$ and other geochemical tracers. Deep Sea Res. Part 1: Oceanogr. Res. Pap. 57 (7), 847–859.

Bostock, H.C., Barrows, T.T., Carter, L., Chase, Z., Cortese, G., Dunbar, G.B., Ellwood, M., et al., 2013. A review of the Australian–New Zealand sector of the

Southern Ocean over the last 30 ka (Aus-INTIMATE project). Quaternary Science Reviews 74, 35–57.
Bradtmiller, L.I., Anderson, R.F., Fleisher, M.Q., Burckle, L.H., 2006. Diatom productivity in the equatorial Pacific Ocean from the last glacial period to the present: a test of the silicic acid leakage hypothesis. Paleoceanography 21. http://dx.doi.org/10.1029/2006PA001282.
Bradtmiller, L.I., Anderson, R.F., Fleisher, M.Q., Burckle, L.H., 2007. Opal burial in the equatorial Atlantic Ocean over the last 30 ka: implications for glacial-interglacial changes in the ocean silicon cycle. Paleoceanography 22. http://dx.doi.org/10.1029/2007PA001443.
Bradtmiller, L.I., Anderson, R.F., Fleisher, M.Q., Burckle, L.H., 2009. Comparing glacial and Holocene opal fluxes in the Pacific sector of the Southern Ocean. Paleoceanography 24. http://dx.doi.org/10.1029/2008PA001693.
Broecker, W.S., Peng, T.-H., 1987. The role of $CaCO_3$ compensation in the glacial to interglacial atmospheric CO_2 change. Glob. Biogeochem. Cycles 1, 15–29.
Brzezinski, M.A., Dumousseaud, C., Krause, J.W., Measures, C.I., Nelson, D.M., 2008. Iron and silicic acid concentrations together regulate Si uptake in the equatorial Pacific Ocean. Limnol. Oceanogr. 53, 875–889.
Brzezinski, M.A., Nelson, D.M., 1996. Chronic substrate limitation of silicic acid uptake rates in the western Sargasso Sea. Deep-Sea Res. II 43, 437–453.
Brzezinski, M.A., Sigman, D.M., Sarmiento, J.L., Matsumoto, K., Gruber, N., Rau, G.H., Coale, K.H., 2002. A switch from $Si(OH)_4$ to NO_3^- depletion in the glacial Southern Ocean. Geophys. Res. Lett. 29, 1564.
Burke, A., Robinson, L.F., 2011. The Southern Ocean's role in carbon exchange during the last deglaciation. Science 335 (6068), 557–561.
Calvo, E., Pelejaro, C., Logan, G.A., Deckker, P., 2004. Dust-induced changes in phytoplankton composition in the Tasman Sea during the last four interglacials. Paleoceanography 19, PA2020.
Calvo, E., Pelejero, C., Pena, L.D., Cacho, I., Logan, G.A., 2011. Eastern Equatorial Pacific productivity and related-CO_2 changes since the last glacial period. Proc. Natl. Acad. Sci. U. S. A. 108, 5537–5541.
Cao, Z., Frank, M., Dai, M., Grasse, P., Ehlert, C., 2012. Silicon isotope constraints on sources and utilization of silicic acid in the northern South China Sea. Geochim. Cosmochim. Acta 97, 88–104.
Cardinal, D., Alleman, L.Y., Dehairs, F., Savoye, N., Trull, T.W., Andre, L., 2005. Relevance of silicon isotopes to Si-nutrient utilization and Si-source assessment in Antarctic waters. Glob. Biogeochem. Cycles 19. http://dx.doi.org/10.1029/2004GB002364.
Cardinal, D., Savoye, N., Trull, T.W., Dehairs, F., Kopczynska, E.E., Fripiat, F., Tison, J.-L., André, L., 2007. Silicon isotopes in spring Southern Ocean diatoms: large zonal changes despite homogeneity among size fractions. Mar. Chem. 106 (1), 46–62.
Chase, Z., Anderson, R.F., Fleisher, M.Q., Kubik, P.W., 2002. The influence of particle composition and particle flux on the scavenging of Th, Pa and Be in the ocean. Earth Planet. Sci. Lett. 204, 215–229.
Chase, Z., Anderson, R.F., Fleisher, M.Q., Kubik, P.W., 2003a. Accumulation of biogenic and lithogenic material in the Pacific sector of the Southern Ocean during the past 40,000 years. Deep-Sea Res. II 50, 799–832.
Chase, Z., Anderson, R.F., Fleisher, M.Q., Kubik, P.W., 2003b. Scavenging of Th-230, Pa-231 and Be-10 in the Southern Ocean (SW Pacific Sector): the importance of particle flux, particle composition and advection. Deep-Sea Res. II: Top. Stud. Oceanogr. 50, 739–768.
Cortese, G., Gersonde, R., Hillendbrand, C.-D., Kuhn, G., 2004. Opal sedimentation shifts in the World Ocean over the last 15 Myr. Earth Planet. Sci. Lett. 224, 509–527.
Crosta, X., Beucher, C., Pahnke, K., Brzezinski, M.A., 2007. Silicic acid leakage from the Southern Ocean: opposing effects of nutrient uptake and oceanic circulation. Geophys. Res. Lett. 34, L13601, 13610.13029/12006GL029083.
De La Rocha, C., Bickle, M., 2005. Sensitivity of silicon isotopes to whole-ocean changes in the silica cycle. Mar. Geol. 217, 267–282.
De La Rocha, C., Brzezinski, M.A., DeNiro, M.J., 1997. Fractionation of silicon isotopes by marine diatoms during biogenic silica formation. Geochim. Cosmochim. Acta 61, 5051–5056.
De La Rocha, C., Brzezinski, M.A., DeNiro, M.J., Shemesh, A., 1998. Silicon isotope composition of diatoms as an indicator of past oceanic change. Nature 395, 680–683.
De La Rocha, C.L., 2003. Silicon isotope fractionation by marine sponges and the reconstruction of the silicon isotope composition of ancient deep water. Geology 31, 423–426.
De La Rocha, C.L., Bescont, P., Croguennoc, A., Ponzevera, E., 2011. The silicon isotope composition of surface waters in the Atlantic and Indian Sectors of the Southern Ocean. Geochim. Cosmochim. Acta 75 (18), 5283–5295.
De La Rocha, C.L., Brzezinski, M.A., DeNiro, M.J., 2000. A first look at the distribution of the stable isotopes of silicon in natural waters. Geochim. Cosmochim. Acta 64, 2467–2477.
de Souza, G.F., Reynolds, B.C., Johnson, G.C., Bullister, J.L., Bourdon, B., 2012a. Silicon stable isotope distribution traces Southern Ocean export of Si to the eastern South Pacific thermocline. Biogeosciences 9, 4199–4213.
de Souza, G.F., Reynolds, B.C., Rickli, J., Frank, M., Saito, M.A., Gerringa, L.J.A., Bourdon, B., 2012b. Southern Ocean control of silicon stable isotope distribution in the deep Atlantic Ocean. Glob. Biogeochem. Cycles 26 (2). http://dx.doi.org/10.1029/2011GB004141.
Demarest, M.S., Brzezinski, M.A., Beucher, C., 2009. Fractionation of silicon isotopes during biogenic silica dissolution. Geochim. Cosmochim. Acta 73, 5572–5583.
DeMaster, D.J., 2002. The accumulation and cycling of biogenic silica in the Southern Ocean: revisiting the marine silica budget. Deep-Sea Res. II 49, 3155–3167.
dos Santos, R.A.L., Wilkins, D., De Deckker, P., Schouten, S., 2012. Late Quaternary productivity changes from offshore Southeastern Australia: a biomarker approach. Palaeogeogr. Palaeoclimatol. Palaeoecol. 363, 48–56.
Dubois, N., Kienast, M., Kienast, S., Calvert, S.E., Francois, R., Anderson, R.F., 2010. Sedimentary opal records in the eastern equatorial Pacific: it's not all about leakage. Glob. Biogeochem. Cycles 24, GB4020, 4010.1029/2010GC003821.
Egan, K., Rickaby, R.E.M., Leng, M.J., Hendry, K.R., Hermoso, M., Sloane, H.J., Bostock, H., Halliday, A.N., 2012. Diatom silicon isotopes as a proxy for silicic acid utilisation: a Southern Ocean core top calibration. Geochim. Cosmochim. Acta 96, 174–192.
Ehlert, C., Grasse, P., Frank, M., 2013. Changes in silicate utilisation and upwelling intensity off Peru since the Last Glacial Maximum – insights from silicon and beodymium isotopes. Quat. Sci. Rev. 72, 18–35.
Ellwood, M.J., Hunter, K.A., 1999. Determination of the Zn/Si ratio in diatom opal: a method for the separation, cleaning and dissolution of diatoms. Mar. Chem. 66, 149–160.
Ellwood, M.J., Wille, M., Maher, W., 2010. Glacial silicic acid concentrations in the Southern Ocean. Science 330, 1088–1091.
Etourneau, J., Ehlert, C., Frank, M., Martinez, P., Schneider, R., 2012. Contribution of changes in opal productivity and nutrient distribution in the coastal upwelling systems to Late Pliocene/Early Pleistocene climate cooling. Clim. Past 8, 1435–1445.
Falkowski, P.G., Katz, M.E., Knoll, A.H., Quigg, A., Raven, J.A., Schofield, O., Taylor, F.J.R., 2004. The evolution of modern eukaryotic phytoplankton. Science 305, 354–360.
Frank, N., Gersonde, R., Rutgers van der Loeff, M.M., Bohrmann, G., Nürnberg, C.C., Kubik, P.W., Suter, M., Mangini, A., 2000. Similar glacial and interglacial export productivity in the Atlantic sector of the Southern Ocean. Multiproxy evidence and implications for glacial atmospheric CO_2. Paleoceanography 15, 642–658.
Fripiat, F., Cardinal, D., Tison, J.-L., Worby, A., André, L., 2007. Diatom-induced silicon isotopic fractionation in Antarctic sea ice. J. Geophys. Res. 112. http://dx.doi.org/10.1029/2006JG000244.
Fripiat, F., Cavagna, A.-J., Dehairs, F., de Brauwere, A., Andre, L., Cardinal, D., 2012. Processes controlling the Si-isotopic composition in the Southern Ocean ad application for paleoceanography. Biogeosciences 9, 2443–2457.
Fripiat, F., Cavagna, A.-J., Savoye, N., Dehairs, F., Andre, L., Cardinal, D., 2011. Isotopic constraints on the Si-biogeochemical cycle of the Antarctic Zone in the Kerguelen area (KEOPS). Mar. Chem. 123 (1–4), 11–22.
Froelich, P.N., Blanc, V., Mortlock, R.A., Chillrud, S.N., 1992. River fluxes of dissolved silica to the ocean were higher during glacials. Ge/Si in diatoms, rivers and oceans. Paleoceanography 7, 739–767.
Georg, R.B., West, A.J., Basu, A.R., Halliday, A.N., 2009. Silicon fluxes and isotope composition of direct groundwater discharge into the Bay of Bengal and the effect on the global ocean silicon budget. Earth Planet. Sci. Lett. 283 (1–4), 67–74.
Griffiths, J.D., Barker, S., Hendry, K.R., Thornalley, D.J.R., van de Flierdt, T., Hall, I.R., Anderson, R.F., 2013. Evidence of silicic acid leakage to the tropical Atlantic via Antarctic intermediate water during marine isotope stage 4. Paleoceanography 28, 307–318.
Gutjahr, M., Frank, M., Stirling, C.H., Keigwin, L.D., Halliday, A.N., 2008. Tracing the Nd isotope evolution of North Atlantic deep and intermediate waters in the western North Atlantic since the Last Glacial Maximum from Blake Ridge sediments. Earth Planet. Sci. Lett. 266 (1–2), 61–77.
Harrison, K.G., 2000. Role of increased marine silica input on paleo-pCO_2 levels. Paleoceanography 15, 292–298.
Hayes, C.T., Anderson, R.F., Fleisher, M.Q., 2011. Opal accumulation rates in the equatorial Pacific and mechanisms of deglaciation. Paleoceanography 26, PA1207, 1210.1029/2010PA002008.
Hendry, K.R., Andersen, M.B., 2013. The zinc isotopic composition of siliceous marine sponges: investigating nature's sediment traps. Chem. Geol. 354, 33–41.
Hendry, K.R., Georg, R.B., Rickaby, R.E.M., Robinson, L.F., Halliday, A.N., 2010. Deep ocean nutrients during the Last Glacial Maximum deduced from sponge silicon isotopic compositions. Earth Planet. Sci. Lett. 292, 290–300.
Hendry, K.R., Leng, M.J., Robinson, L.F., Sloane, H.J., Blusztjan, J., Rickaby, R.E.M., Georg, R.B., Halliday, A.N., 2011. Silicon isotopes in Antarctic sponges: an interlaboratory comparison. Antarct. Sci. 23, 34–42.
Hendry, K.R., Rickaby, R.E.M., 2008. Opal (Zn/Si) ratios as a nearshore geochemical proxy in coastal Antarctica. Paleoceanography 23, PA2218. http://dx.doi.org/10.1029/2007PA001576.
Hendry, K.R., Robinson, L.F., 2012. The relationship between silicon isotope fractionation in sponges and silicic acid concentration: modern and core-top studies of biogenic opal. Geochim. Cosmochim. Acta 81, 1–12.
Hendry, K.R., Robinson, L.F., McManus, J.F., Hays, J.D., 2014. Silicon isotopes indicate enhanced carbon export efficiency in the North Atlantic during deglaciation. Nat. Commun. 5, 3107. http://dx.doi.org/10.1038/ncomms4107.
Hendry, K.R., Robinson, L.F., Meredith, M.P., Mulitza, S., Chiessi, C.M., Arz, H., 2012. Abrupt changes in high-latitude nutrient supply to the Atlantic during the last glacial cycle. Geology 40 (2), 123–126.
Higginson, M.J., Altabet, M.A., 2004. Initial tests of the silicic acid leakage hypothesis using sedimentary biomarkers. Geophys. Res. Lett. 31, L18303, 18310.11029/12004GL020511.

Holte, J., Talley, L.D., Chereskin, T.K., Sloyan, B.M., 2012. The role of air-sea fluxes in Subantarctic Mode Water formation. J. Geophys. Res. 117, C03040. http://dx.doi.org/10.1029/2011JC007798.
Horn, M.G., Beucher, C., Robinson, R.S., Brzezinski, M.A., 2011. Southern Ocean nitrogen and silicon dynamics during the last deglaciation. Earth Planet. Sci. Lett. 310, 334–339.
Hutchins, D.A., DiTullio, G.R., Zhang, Y., Bruland, K.W., 1998. An iron limitation mosaic in the California upwelling regime. Limnol. Oceanogr. 43 (6), 1037–1054.
Johnson, H.P., Hautala, S.L., Bjorklund, T.A., Zarnetske, M.R., 2006. Quantifying the North Pacific silica plume. Geochem. Geophys. Geosystems 7, Q05011, 05010.01029/02005GC001065.
Keigwin, L.D., 2004. Radiocarbon and stable isotope constrainst on Last Glacial Maximum and Younger Dryas ventilation in the western North Atlantic. Paleoceanography 19, PA4012, 4010.1029/2004PA001029.
Kemp, A.E.S., Pearce, R.B., Grigorov, I., Rance, J., Lange, C.B., Quilty, P., Salter, I., 2006. Production of giant marine diatoms and their export at oceanic frontal zones: implications for Si and C flux from stratified oceans. Glob. Biogeochem. Cycles 20. http://dx.doi.org/10.1029/2006GB002698.
Kienast, S.S., Kienast, M., Jaccard, S., Calvert, S.E., Francois, R., 2006. Testing the silica leakage hypothesis with sedimentary opal records from the eastern equatorial Pacific over the last 150 kyrs. Geophys. Res. Lett. 33, L15607, 15610.11029/12006GL026651.
Koutavas, A., Sachs, J.P., 2008. Northern timing of deglaciation in the eastern equatorial Pacific from alkenone paleothermometry. Paleoceanography 23. http://dx.doi.org/10.1029/2008PA001593.
Kumar, N., Anderson, R.F., Mortlock, R.A., Froelich, P.N., Kubik, P., Dittrich-Hannen, B., Suter, M., 1995. Increased biological productivity and export production in the glacial Southern Ocean. Nature 378, 675–680.
Lal, D., Charles, C., Vacher, L., Goswami, J.N., Jull, A.J.T., McHargue, L., Finkel, R.C., 2006. Paleo-ocean chemistry records in marine opal: implications for fluxes of trace elements, cosmogenic nuclides (^{10}Be and ^{26}Al), and biological productivity. Geochim. Cosmochim. Acta 70, 3275–3289.
Lambert, F., Delmonte, B., Petit, J.R., Bigler, M., Kaufmann, P.R., Hutterli, M.A., Stocer, T.F., Ruth, U., Steffensen, J.P., Maggi, V., 2008. Dust-climate couplings over the past 800,000 years from the EPICA Dome C ice core. Nature 452, 616–619.
Leng, M.J., Sloane, H.J., 2008. Combined oxygen and silicon isotope analysis of biogenic silica. J. Quat. Sci. 23, 313–319.
Maldonado, M., Navarro, L., Grasa, A., Gonzalez, A., Vaquerizo, I., 2011. Silicon uptake by sponges: a twist to understanding nutrient cycling on continental margins. Nat. Sci. Reports 1. http://dx.doi.org/10.1038/srep00030.
Mangini, A., Godoy, J.M., Godoy, M.L., Kowsman, R., Santos, G.M., Ruckelshausen, M., Schroeder-Ritzrau, A., Wacker, L., 2010. Deep sea corals off Brazil verify a poorly ventilated Southern Pacific Ocean during H1 and the Younger Dryas. Earth Planet. Sci. Lett. 293, 269–276.
Marchetti, A., Harrison, P.J., 2007. Coupled changes in the cell morphology and the elemental (C, N and Si) composition of the pennate diatom *Pseudo-nitzschia* due to iron deficiency. Limnol. Oceanogr. 52 (5), 2270–2284.
Marinov, I., Gnanadesikan, A., Sarmiento, J.L., Toggweiler, J.R., Follows, M., Mignone, B.K., 2008. Impact of oceanic circulation on biological carbon storage in the ocean and atmospheric pCO2. Glob. Biogeochem. Cycles 22, GB3007, 3010.1029/2007GB002958.
Marinov, I., Gnanadesikan, A., Toggweiler, R., Sarmiento, J.L., 2006. The southern ocean biogeochemical divide. Nature 441, 964–968.
Martin-Jezequel, V., Hildebrand, M., Brzezinksi, M.A., 2003. Silicon metabolism in diatoms: implications for growth. J. Phycol. 36 (5), 821–840.
Marshall, J., Speer, K., 2012. Closure of the meridional overturning circulation through Southern Ocean upwelling. Nat. Geosci. 5, 171–180.
Matsumoto, K., Sarmiento, J.L., 2008. A corollary to the silicic acid leakage hypothesis. Paleoceanography 23. http://dx.doi.org/10.1029/2007PA001515.
Matsumoto, K., Sarmiento, J.L., Brzezinski, M.A., 2002. Silicic acid leakage from the Southern Ocean: a possible explanation for glacial atmospheric pCO_2. Glob. Biogeochem. Cycles 16, 1031.
McClymont, E.L., Ganeshram, R.S., Pichevin, L.E., Talbot, H.M., van Dongen, B.E., Thunell, R.C., Haywood, A.M., Singarayer, J.S., Valdes, P.J., 2012. Sea-surface temperature records of termination I in the Gulf of California: challenges for seasonal and interannual analogies of tropical Pacific climate change. Paleoceanography 27. http://dx.doi.org/10.1029/2011PA002226.
McManus, J.F., Francois, R., Gherardi, J.-M., Keigwin, L.D., Brown-Leger, S., 2004. Collapse and rapid resumption of Atlantic meridional circulation linked to deglacial climate changes. Nature 428, 834–837.
Meckler, A.N., Sigman, D.M., Gibson, K.A., Francois, R., Martinez-Garcia, A., Jaccard, S.L., Rohl, U., Peterson, L.C., Tiedemann, R., Haug, G.H., 2013. Deglacial pulses of deep-ocean silicate into the subtropical North Atlantic Ocean. Nature 495, 495–498.
Milligan, A.J., Varela, D.E., Brzezinski, M.A., Morel, F.M.M., 2004. Dynamics of silicon metabolism and silicon isotopic discrimination in a marine diatom as a function of pCO_2. Limnol. Oceanogr. 49, 322–329.
Minoletti, F., Hermoso, M., Gressier, V., 2009. Separation of sedimentary micron-sized particles for palaeoceanography and calcareous nannoplankton biogeochemistry. Nat. Protoc. 4, 14–24.
Moreno, A., Nave, S., Kuhlmann, H., Canals, M., Targarona, J., Freudenthal, T., Abrantes, F.G., 2002. Productivity response in the North Canary Basin to climate changes during the last 250,000 yr: a multi-proxy approach. Earth Planet. Sci. Lett. 196 (3–4), 147–159.
Nelson, D.M., Anderson, R.F., Barber, R.T., Brzezinski, M.A., Buesseler, K.O., Chase, Z., Collier, R.W., Dickson, M.-L., Francois, R., Hiscock, M.R., Honjo, S., Marra, J., Martin, W.R., Sambrotto, R.N., Sayles, F.L., Sigman, D.E., 2002. Vertical budgets for organic carbon and biogenic silica in the Pacific sector of the Southern Ocean, 1996–1998. Deep-Sea Res. II 49, 1645–1674.
Nelson, D.M., Treguer, P., Brzezinski, M.A., Leynaert, A., Queguiner, B., 1995. Production and dissolution of biogenic silica in the ocean: revised global estimates, comparison with regional data and relationship to biogenic sedimentation. Glob. Biogeochem. Cycles 9, 359–372.
Nozaki, Y., Yamamoto, Y., 2001. Radium 228 based nitrate fluxes in the eastern Indian Ocean and the South China Sea and silica-induced "alkalinity pump" hypothesis. Glob. Biogeochem. Cycles 15, 555–567.
Opfergelt, S., Burton, K.W., Pogge von Strandmann, P.A.E., Gislason, S.R., Halliday, A.N., 2013. Riverine silicon isotope variations in glaciated basaltic terrains: implications for the Si delivery to the ocean over glacial-interglacial intervals. Earth Planet. Sci. Lett. 369-370, 211–219.
Pahnke, K., Zahn, R., 2005. Southern Hemisphere water mass conversion linked with North Atlantic climate variability. Science 307, 1741–1746.
Pahnke, K., Goldstein, S.L., Hemming, S.R., 2008. Abrupt changes in Antarctic Intermediate Water circulation over the past 25,000 years. Nat. Geosci. 1, 870–874.
Pena, L., Goldstein, S.L., Hemming, S.R., Jones, K.M., Calvo, E., Pelejero, C., Cacho, I., 2013. Rapid changes in meridional advection of Southern Ocean intermediate waters to the tropical Pacific during the last 30 kyr. Earth Planet. Sci. Lett. 368, 20–32.
Pichat, S., Sims, K.W.W., Francois, R., McManus, J.F., Leger, S.B., Albarede, F., 2004. Lower export production during glacial periods in the equatorial Pacific from $(^{231}Pa/^{230}Th)_{xs,0}$ measurements in deep-sea sediments. Paleoceanography 19, PA4023, 4010.1029/2003PA000994.
Pichevin, L.E., Ganeshram, R.S., Francavilla, S., Arellano-Torres, E., Pedersen, T.F., Beaufort, L., 2010. Interhemispheric leakage of isotopically heavy nitrate in the eastern tropical Pacific during the last glacial period. Paleoceanography 25, PA1204, 1210.1029/2009PA001754.
Pichevin, L.E., Reynolds, B.C., Ganeshram, R.S., Cacho, I., Pena, L., Keefe, K., Ellam, R.M., 2009. Enhanced carbon pump inferred from relaxation of nutrient limitation in the glacial ocean. Nature 459, 1114–1117.
Piotrowski, A.M., Goldstein, S.L., Hemming, S.R., Fairbanks, R.G., Zylberberg, D.R., 2008. Oscillating glacial northern and southern deep water formation from combined neodymium and carbon isotopes. Earth Planet. Sci. Lett. 272, 394–405.
Pondaven, P., Ragueneau, O., Tréguer, P., Hauvespre, A., Dezileau, L., Reyss, J.L., 2000. Resolving the "opal paradox" in the Southern Ocean. Nature 405, 168–172.
Reincke, T., Barthel, D., 1997. Silica uptake kinetics of *Halichondria panicea* in Kiel Bight. Mar. Biol. 129, 591–593.
Ren, H., Brunelle, B.G., Sigman, D.M., Robinson, R.S., 2013. Diagenetic aluminium uptake into diatom frustules and the preservation of diatom-bound organic nitrogen. Mar. Chem. 155, 92–102.
Reynolds, B.C., 2009. Modeling the modern marine δ^{30}Si distribution. Glob. Biogeochem. Cycles 23, GB2015, 2010.1029/2008GB003266.
Reynolds, B.C., Frank, M., Halliday, A.N., 2006. Silicon fractionation during nutrient utilization in the North Pacific. Earth Planet. Sci. Lett. 244, 431–443.
Richaud, M., Loubere, P., Pichat, S., Francois, R., 2007. Changes in opal flux and the rain ratio during the last 50,000 years in the equatorial Pacific. Deep-Sea Res. II: Top. Stud. Oceanogr. 54 (5–7), 762–771.
Rickaby, R.E.M., Bard, E., Sonzogni, C., Rostek, F., Beaufort, L., Barker, S., Rees, G., Schrag, D.P., 2007. Coccolith chemistry reveals secular variations in the global ocean carbon cycle? Earth Planet. Sci. Lett. 253 (1–2), 83–95.
Roberts, N.L., Piotrowski, A.M., McManus, J.F., Keigwin, L.D., 2010. Synchronous deglacial overturning and water mass source changes. Science 327, 75–78.
Robinson, L.F., Adkins, J.F., Keigwin, L.D., Southon, J., Fernandez, D.P., Wang, S.-L., Scheirer, D.S., 2005a. Radiocarbon variability in the western North Atlantic during the last deglaciation. Science 310, 1469–1473.
Robinson, R.S., Brunelle, B.G., Sigman, D.M., 2004. Revisiting nutrient utilization in the glacial Antarctic: evidence from a new method for diatom-bound N isotope analysis. Paleoceanography 19. http://dx.doi.org/10.1029/2003PA000996.
Robinson, R.S., Sigman, D.M., DiFiore, P.J., Rohde, M.M., Mashiotta, T.A., Lea, D.W., 2005b. Diatom-bound $^{15}N/^{14}N$: new support for enhanced nutrient consumption in the ice age subantarctic. Paleoceanography 20 (3). http://dx.doi.org/10.1029/2004PA001114.
Romero, O.E., 2010. Changes in style and intensity of production in the Southeastern Atlantic over the last 70,000 yr. Mar. Micropaleontol. 74 (1–2), 15–28.
Romero, O.E., Kim, J.-H., Donner, B., 2008. Submillenial-to-millenial variability of diatom production off Mauritania, NW Africa, during the last glacial cycle. Paleoceanography 23, PA3218, 3210.1029/2008PA001601.
Romero, O.E., Leduc, G., Vidal, L., Fischer, G., 2011. Millennial variability and long-term changes of the diatom population in the eastern equatorial Pacific during the last glacial cycle. Paleoceanography 26. http://dx.doi.org/10.1029/2010PA002099.
Sarmiento, J.L., Gruber, N., Brzezinski, M.A., Dunne, J.P., 2004. High-latitude controls of thermocline nutrients and low latitude biological productivity. Nature 427, 56–60.
Shemesh, A., 1989. Late Cenozoic Ge/Si record of marine biogenic opal: implications for variations of riverine fluxes to the ocean. Paleoceanography 4, 221–234.
Shemesh, A., 1995. Late Pleistocene oxygen isotope records of biogenic silica from the Atlantic sector of the Southern Ocean. Paleoceanography 10, 179–196.
Sigman, D.M., Hain, M.P., Haug, G.H., 2010. The polar ocean and glacial cycles in atmospheric CO_2 concentration. Nature 466, 47–55.

Spero, H.J., Lea, D.W., 2002. The cause of carbon isotope minimum events on glacial terminations. Science 296, 522–525.
Sutton, J., Varela, D., Brzezinski, M.A., Beucher, C., 2013. Species-dependent silicon isotope fractionation by marine diatoms. Geochim. Cosmochim. Acta 104, 300–309.
Takeda, S., 1998. Influence of iron availability on nutrient consumption ratio of diatoms in oceanic waters. Nature 393 (6687), 774–777.
Thornalley, D.J.R., Barker, S., Broecker, W.S., Elderfield, H., McCave, I.N., 2011. The deglacial evolution of North Atlantic deep convection. Science 331 (6014), 202–205.
Toggweiler, R., 1999. Variation of atmospheric CO_2 by ventilation of the ocean's deepest water. Paleoceanography 14, 571–588.
Tréguer, P., De la Rocha, C.L., 2013. The world ocean silica cycle. Annu. Rev. Mar. Sci. 5, 477–501.
Tréguer, P., Nelson, D.M., Van Bennekom, A.J., DeMaster, D.J., Leynaert, A., Quéguiner, B., 1995. The silica balance in the world ocean: a re-estimate. Science 268, 375–379.
Varela, D.E., Pride, C.J., Brzezinski, M.A., 2004. Biological fractionation of silicon isotopes in Southern Ocean surface waters. Glob. Biogeochem. Cycles 18. http://dx.doi.org/10.1029/2003GB002140.
Vink, A., Ruhlemann, C., Zonneveld, K.A.F., Mulitza, S., Huls, M., Willems, H., 2001. Shifts in the position of the North Equatorial current and rapid productivity changes in the western Tropical Atlantic during the last glacial. Paleoceanography 16 (5), 479–490.
Wetzel, F., de Souza, G.F., Reynolds, B.C., 2014. What controls silicon isotope fractionation during dissolution of diatom opal? Geochim. Cosmochim. Acta (in press).
Wille, M., Sutton, J., Ellwood, M.J., Sambridge, M., Maher, W., Eggins, S., Kelly, M., 2010. Silicon isotopic fractionation in marine sponges: a new model for understanding silicon isotopic fractionation in sponges. Earth Planet. Sci. Lett. 292. http://dx.doi.org/10.1016/j.epsl.2010.1001.1036.
Wischmeyer, A.G., De La Rocha, C., Maier-Raimer, E., Wolf-Gladrow, D.A., 2003. Control mechanisms for the oceanic distribution of silicon isotopes. Glob. Biogeochem. Cycles 17. http://dx.doi.org/10.1029/2002GB002022.
Wu, S., Ding, T., Meng, X., Bai, L., 1997. Determinaton and geological implication of O-Si isotope of the sediment core in the CC area, the Pacific Ocean. Chin. Sci. Bull. 42, 1462–1465.
Xie, R.C., Marcantonio, F., Schmidt, M.W., 2012. Deglacial variability of Antarctic Intermediate Water penetration into the North Atlantic from authigenic neodymium isotope ratios. Paleoceanography 27 (3). http://dx.doi.org/10.1029/2012/PA002337.
Xiong, Z., Li, T., Crosta, X., Algeo, T., Chang, F., Zhai, B., 2013. Potential role of giant marine diatoms in sequestration of atmsopheric CO_2 during the Last Glacial Maximum: $\delta^{13}C$ evidence from laminated *Ethmodiscus rex* mats in tropical West Pacific. Glob. Planet. Change 108, 1–14.
Zhai, B., Li, T., Chang, F., Cao, Z., 2009. Vast laminated diatom mat deposits from the west low-latitude Pacific Ocean in the last glacial period. Chin. Sci. Bull. 54 (23), 4529–4533.
Ziegler, K., Chadwick, O.A., Brzezinski, M.A., Kelly, E.F., 2005. Natural variations of $\delta^{30}Si$ ratios during progressive basalt weathering, Hawaiian Islands. Geochim. Cosmochim. Acta 69 (19), 4597–4610.